


3D bioprinting for skin tissue engineering: Current status and perspectives

Journal of Tissue Engineering
Volume 12: 1–28
© The Author(s) 2021
Article reuse guidelines:
sagepub.com/journals-permissions
DOI: 10.1177/20417314211028574
journals.sagepub.com/home/tej



Tingting Weng^{1,2}, Wei Zhang^{1,2}, Yilan Xia¹, Pan Wu^{1,2},
Min Yang^{1,2}, Ronghua Jin^{1,2}, Sizhan Xia^{1,2}, Jialiang Wang^{1,2},
Chuangang You^{1,2}, Chunmao Han^{1,2} and Xingang Wang^{1,2} 

Abstract

Skin and skin appendages are vulnerable to injury, requiring rapidly reliable regeneration methods. In recent years, 3D bioprinting has shown potential for wound repair and regeneration. 3D bioprinting can be customized for skin shape with cells and other materials distributed precisely, achieving rapid and reliable production of bionic skin substitutes, therefore, meeting clinical and industrial requirements. Additionally, it has excellent performance with high resolution, flexibility, reproducibility, and high throughput, showing great potential for the fabrication of tissue-engineered skin. This review introduces the common techniques of 3D bioprinting and their application in skin tissue engineering, focusing on the latest research progress in skin appendages (hair follicles and sweat glands) and vascularization, and summarizes current challenges and future development of 3D skin printing.

Keywords

3D bioprinting, skin, skin appendages, tissue engineering, regenerative medicine

Date received: 26 March 2021; accepted: 10 June 2021

Introduction

Skin, as the largest organ in direct contact with the outside world. There is no doubt that skin is also the most vulnerable organ. Although skin has higher regeneration ability than most tissues, the repair of large-scale deep injuries, such as deep burns, is mainly scar repair.¹ The original cellular environment cannot be completely repaired, resulting in the inability to regenerate hair follicles and sweat glands, which greatly impairs prognosis and life quality of patient. For example, in a high-temperature environment, patients who lack sweat glands cannot regulate their body temperature through perspiration, leading to hyperthermia, heat stroke, and even death.² Deep burns destroy a large number of hair follicles, which greatly affects personal appearance and may lead to psychological diseases such as depression.

To date, the most used treatment for skin defects is autologous skin transplantation. However, the shortage of donor sites, secondary injuries, and infection risk limit the

application of autologous skin transplantation. Compared with traditional treatment methods, skin tissue engineering (STE) provides a novel approach to treat skin defects. Various types of tissue-engineered skin (TES) have been developed, such as Integra, Dermagraft, and PELNAC.³ TES is mainly composed of biomaterials, cells, and bioactive factors. It can completely cover skin wounds, accelerating wound healing with less scar and promoting the vascularization of dermal substitutes.⁴ However, there are

¹Department of Burns & Wound Care Centre, The Second Affiliated Hospital of Zhejiang University School of Medicine, Hangzhou, Zhejiang, China

²The Key Laboratory of Trauma and Burns of Zhejiang University, Hangzhou, Zhejiang, China

Corresponding author:

Xingang Wang, Department of Burns & Wound Care Center, The Second Affiliated Hospital of Zhejiang University School of Medicine, No. 88, Jiefang Road, Hangzhou, Zhejiang 310009, China.
Email: wangxingang8157@zju.edu.cn



still many limitations of TES, such as non-pigmented skin, insufficient elasticity of dermis, long-term postoperative scars, loss of skin appendages,⁵ and malfunctional nerve recovery,⁶ which negatively affect the quality of life of patients after wound healing. Therefore, the regeneration of skin and appendages are an urgent problem to be solved in the field of tissue engineering (TE) and regenerative medicine.⁷ With the continued development of three-dimensional (3D) printing technology, its accuracy and high resolution has allowed us to print functional skin and appendages. Therefore, these limitations of TES will likely be resolved.

Traditional artificial deposition methods include electrospinning, fiber deposition, freeze-drying, and salt leaching.^{8,9} Electrospinning is the most versatile fabrication method. Compared to conventional dressings and hydrogels, Electrospun nanofibrous materials present remarkable property as dermal substitutes, due to their permission of structures that closely resemble the native extracellular matrix (ECM) of the skin, where cells can adhere, proliferate, infiltrate the scaffold, and induce neoderms regeneration.^{10,11} Recently, *in situ* deposition of electrospun fibers using hand-held electrospinning devices has been used as a promising alternative to conventional electrospinning.^{12,13} In this way, the fibers are directly deposited on the impaired tissue to promote tissue repair and regeneration. In addition, 3D nanofiber structures fabricated by wet electrospinning and multilayering provide the advantage of morphological control with tunability of scaffold porosity and fiber size.¹⁴

Compared with the traditional artificial deposition method, 3D bioprinting has some advantages in TES preparation, including: (1) According to the shape and depth of the wound surface, the computer scanning imaging technology can quickly print out the skin graft matched with the wound, which has the characteristics of timeliness, high flux, and high repeatability.^{15,16} (2) Multiple bioinks are available. They can flexibly and accurately deposit different biological agents (including living cells, nucleic acids, growth factors, and pregelatinized solutions, etc.) to construct tissue structures, which exhibit morphology and physiology similar to that of normal skin.¹⁷ (3) Using the principle of layer-by-layer deposition, skin tissue can be printed *in situ* on the wound surface.¹⁸ (4) 3D-bioprinted constructs with interconnected pores and large surface areas support cell attachment, growth, intercellular communication, and exchange of gas and nutrients, a notable advantage over traditional solvent casting, phase separation, and melt molding techniques.¹⁹ Over the past decade, 3D bioprinting technology has been used for the manufacture of biological tissues in various fields, such as vascular systems, heart, bone, cartilage, skin, and liver.²⁰ At present, 3D bioprinting technology has attracted increasing attention based on its immense potential for the development of TES (Figure 1).

Structure and functions of skin and appendages

Skin

Skin is the largest organ of the body, accounting for about 16% of the total body weight in adults.²¹ The skin is composed of epidermis, dermis, and subcutaneous tissue (Figure 2). The constituents and functions of the three layers are summarized in Table 1. The epidermis is the outermost layer, consisting of keratinocytes (KCs), and contains no blood vessels.²² The epidermis can be divided into five layers from the basal layer to the surface; namely, the stratum basale, the stratum spinosum, the stratum granulosum, the stratum lucidum, and the stratum corneum.²³ Four different cell types reside in these layers of the epidermis: KCs, melanocytes (MCs), Langerhans cells, and Merkel cells. The middle layer is the dermis, which is much thicker than the epidermis, and can be divided into papillary dermis and reticular dermis.²⁴ Blood vessels and nerves pass through the dermis to provide nutrition and sensation. Various appendages can also be found in this layer, including sweat glands, hair follicles, and sebaceous glands. The innermost layer is subcutaneous tissue, composed of adipocytes and collagen. It can resist cold, buffer deep tissues from severe trauma, provide buoyancy, store energy, and can even function as an endocrine organ.²⁵ The skin can protect tissues against external stimulation, prevent invasion of microorganisms, and prevent extravasation of body fluids and absorption of external substances. In addition, the skin has functions such as immune regulation, body temperature regulation, and sensing of external stimuli.^{26,27}

Skin appendages

Skin appendages include hair follicles, sebaceous glands, and sweat glands. For skin 3D printing, few studies have explored the regeneration of sebaceous glands. Therefore, this review mainly introduces the structure, function, and bioprinting research progress of hair follicles and sweat glands.

Hair follicles reside in the dermal layer of the skin and are made up of hair papillae, hair matrix, root sheath, and hair bulges. The papilla is a large structure at the base of the hair follicle, which is mainly composed of connective tissue and a capillary loop. The papilla is a key part of hair follicle,²⁸ which determines the length, hardness, and growth cycle of hair. The root sheath is composed of an external and internal root sheath. The bulge is located in the outer root sheath at the insertion point of the arrector pili muscle. It houses several types of stem cells, which supplies the entire hair follicle with new cells and plays a role in healing the injured epidermis.^{29,30} Hair follicles are widely distributed throughout the body, with only a few

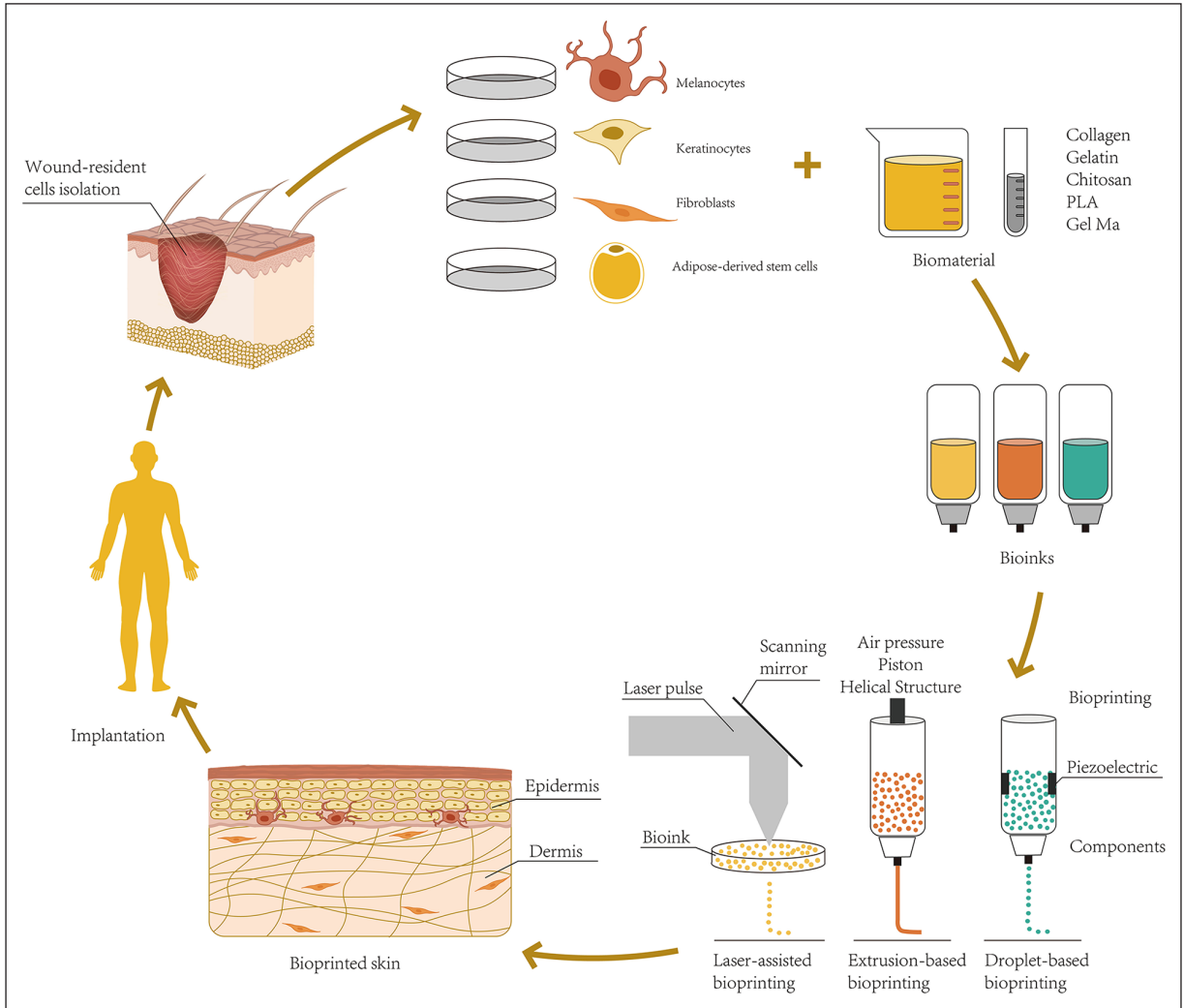


Figure 1. Schematic representation of skin 3D bioprinting.

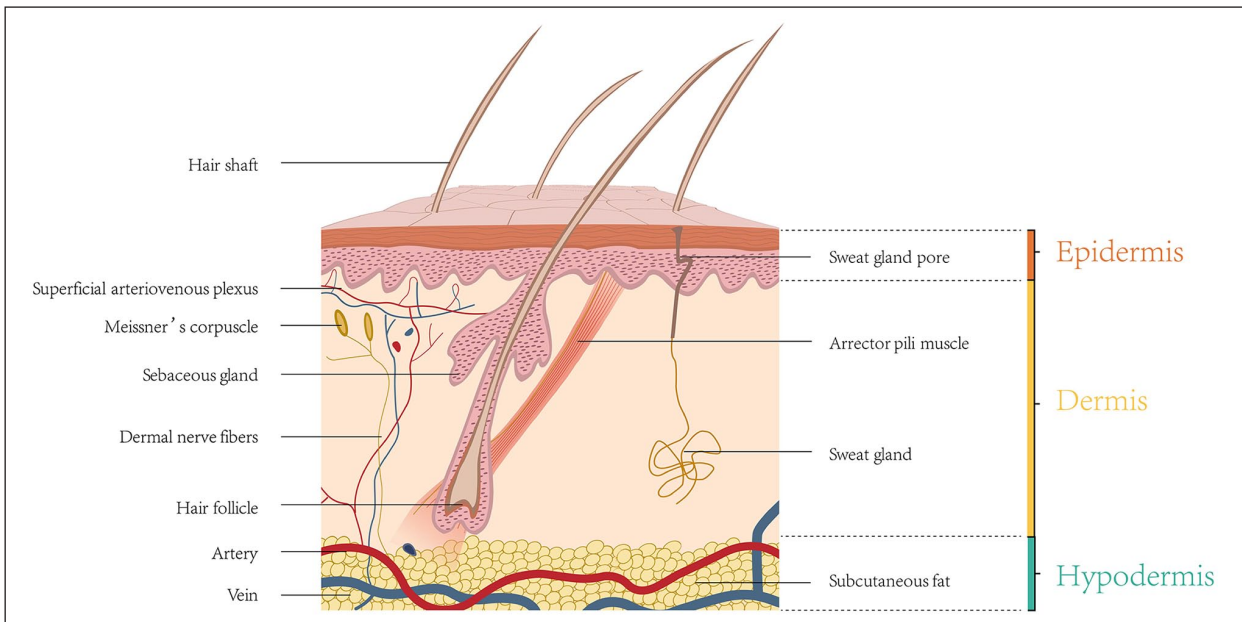


Figure 2. Schematic representation of the skin structure.

Table 1. Constituents and functions of the layers of skin.

	Locations	Functions
Epidermis		
Keratinocytes	Full layer of epidermis	Synthesize keratin, constitutes the skin barrier
Melanocytes	Stratum basale	Production of melanosomes
Merkel cells	Stratum basale	Sensor
Langerhans cells	Stratum spinosum	Antigen-presenting cells, serving an immunologic role
Laminin	Basement membrane	Connect dermis and epidermis
Dermis		
Fibroblasts	Full layer of dermis	Synthesize ECM, secrete various cytokines, and promote wound repair
Collagen fibers	Full layer of dermis	Supporting and protecting function
Elastic fibers	The reticular dermis	Skin elasticity
Blood vessels	The papillary dermis	Supply oxygen and nutrients to skin
Nerves	Along arterioles and venules	Touch, pressure, temperature, itch, and pain sensation
Sweat glands	The reticular dermis	Regulate body temperature
Hair follicle	The reticular dermis	Form physical barrier, antibacterial, inhibit scar formation
Hypodermis		
Adipocytes	Beneath the dermis and above the muscle	Insulate from the cold and violent trauma, provides buoyancy, storing energy
Fibroblasts	Hypodermis	Synthesize ECM, secrete various cytokines, and promote wound repair
Macrophages	Hypodermis	Phagocytosis, adaptive immunity, wound healing

exceptions, such as the palmoplantar skin, lips, and glans penis.³¹ Hair follicles are important accessory organs of the skin, with a unique structure and ability to periodically regenerate. In addition to forming a physical barrier, hair follicles may exhibit antibacterial ability and inhibit scar formation.

Eccrine sweat glands play an important role in regulating body temperature.³² They can be found all over the body, especially in the palms and soles.³³ Eccrine sweat glands are composed of coiled secretory portion and long duct that courses through the dermis to open into the epidermis. They can be activated by either thermal or emotional stimuli and excrete sweat onto the surface of the skin. There are also various proteolytic enzymes³⁴ and active interleukin-1^{35,36} in sweat, which are believed to contribute to the barrier function of the skin. Exocrine sweat glands not only take part in maintaining body temperature, but also produce urea, lactic acid, and creatine, thus inhibiting the growth of bacteria on the skin surface.³⁷

Besides hair follicles and sweat glands, skin color is one of the important skin accessory functions. Skin color is mainly related to MCs, which are located in the basal layer of the epidermis and can produce melanin stored in melanosomes. The melanosomes are excreted into the ECM and then transported to surrounding KCs to protect the skin from UV damage.^{25,38,39} Studies have shown that KCs have a certain regulatory effect on MCs. When KCs and MCs are co-cultured, the growth factors secreted by KCs can promote the proliferation, differentiation, and migration of MCs.^{39,40} In addition, the basement membrane at the dermoepidermal junction can regulate the uptake of tyrosine by MCs.⁴¹ Therefore, the addition of

MCs in the process of 3D skin bioprinting may address the non-pigmented problem.

3D bioprinting technology

3D bioprinting is the utilization of rapid prototyping technologies to print cells, growth factors, and other biomaterials in a layer-by-layer fashion to produce biomedical components that maximally imitate natural tissue/organ characteristics.⁴² Bioprinting is an extended application of rapid prototyping or an additive manufacturing (AM) technique.⁴³ AM generates complex 3D biocompatible structures via automated deposition of biological substances on a substrate using computer-aided design/computer-aided manufacturing (CAD/CAM) technology. According to the different molding principles and printing materials, 3D bioprinting technologies can be roughly divided into droplet-based bioprinting (DBB), extrusion-based bioprinting (EBB), and photocuring-based bioprinting (PBB).⁴⁴ This part will focus on the introduction of several 3D bioprinting technologies, which are widely used in clinical and scientific research.

Droplet based bioprinting (DBB)

DBB technology mainly includes Inkjet bioprinting (IJB), Electrohydrodynamic (EHD) jetting bioprinting, Laser-assisted bioprinting (LAB). IJB can be divided into continuous inkjet (CIJ) printing and drop-on-demand (DOD) printing. Briefly, CIJ printing relies on the inherent tendency of a liquid stream flow to continuously disperse ink droplets with conductivity. By contrast, DOD printing

generates drops of bioink over the substrate when required. CIJ-based bioprinters generate drops at a much faster rate than DOD systems. Compared with CIJ, DOD is suitable for material deposition and patterning due to its high precision and minimal waste of bioink.⁴⁵ DOD mainly uses piezoelectric, thermal, or electrostatic forces to generate droplets, which can flexibly and accurately deposit different biological materials to build a spatially heterogeneous tissue structure.⁴⁶ Its non-contact printing mode is more suitable for in situ biological printing. Some studies have used DOD technology to directly print bioink with human KCs and Fbs on full-thickness skin defects on the back of athymic mice. Compared with the control group without any biological dressing, the skin grafts in the experimental group promoted wound healing and the skin contracture phenomenon was reduced.⁴⁷ However, DOD has some limitations. First, its ink-jet aperture is extremely small (10–150 μm), which is easily blocked by biological materials. Only low viscosity hydrogel or other low concentration biological agents can be applied to DOD.⁴⁸ Second, TES produced by DOD printing generally has no porous structure, which is not conducive to tissue perfusion and substance exchange and limits its clinical application. EHD jetting bioprinting uses an electric field to pull bioink droplets through an orifice, causing bioink droplets to be ejected.⁴⁹ Therefore, electric field strength (applied voltage), flow rate of bioink, and bioink characteristics (including cell type and concentration⁵⁰) can determine printing methods^{49,51} and cell viability.⁵² EHD jetting bioprinting is suitable for bioprinting of highly concentrated bioink (volume weight up to 20%).⁵³

Laser-assisted bioprinting (LAB)

The LAB system consists of four parts, including a pulsed laser source, a laser focusing tool, a laser energy absorbing metallic ribbon film, and a receiving substrate.^{20,54} The LAB technology emits laser light through a pulsed laser source. The laser light is focused on the metal film on the back of the silicate glass and heated locally, so that the bioink deposited on the glass rapidly evaporates and is sprayed onto the substrate in the form of liquid drops.^{55,56} LAB mainly uses a nanosecond laser with ultraviolet or near-ultraviolet wavelengths as an energy source, and its printing resolution can reach the picogram level.⁵⁷ Michael et al.⁵⁸ created a Graftskin skin substitute using LAB technology, which was a major victory in the field of LAB. Koch et al.⁵⁹ used laser printing based on laser-induced forward transfer (LIFT) to print cells derived from skin cell lines (Fbs: NIH-3T3/KCs: HaCaT) and human mesenchymal stem cells (hMSCs). All cell types maintain their ability to proliferate after LIFT, and skin cells and hMSCs show ~98% and ~90% cell survival, respectively. LAB equipment has no nozzle, performs non-contact printing, and can print cells with high activity

and high resolution.^{60–62} However, LAB still lacks a suitable rapid gelation mechanism, which limits its realization of high throughput printing.

Extrusion-based bioprinting (EBB)

EBB technology achieves highly controllable printing through fluid distribution systems and automated machine systems.⁶³ Under the control of a computer, the bioink containing cells passes through a micro-nozzle in the form of continuous filaments using pneumatic, piston, or screw drive approaches. After printing layer by layer, a complete 3D construct is formed.⁶⁴ Hydrogels with shear thinning characteristics perform best in pneumatic-based extrusion bioprinting because they can maintain the state of filaments after extrusion. The screw-driven structure can achieve high-viscosity bioink printing,⁶⁵ which is conducive to the production of more stable 3D-bioprinted tissue. Recent extrusion bioprinters are equipped with multiple printer heads that allow for simultaneous deposition of different bioinks with minimal cross-contamination.⁶⁶ Furthermore, they permit better control over porosity, shape, and cell-distribution in the printed construct. Compared with DBB and LAB, the advantages of EBB include faster printing speed, more types of printable bioink (including cell clumps, high viscosity hydrogels, microcarriers, and acellular matrix components), and better mechanical strength of the printed products. More importantly, EBB can print a porous grid structure, promote the circulation of nutrients and metabolites, and achieve bionic effects. EBB is highly versatile and most suited to fabricate scaffolds or prosthetic implants for TE.⁶⁷ However, EBB has a lower resolution. The minimum resolution usually exceeds 100 μm .^{66,68}

Stereolithography apparatus (SLA)

SLA, a type of bioprinting method that uses photopolymers to generate photopolymerization under precisely controlled light and then solidifies and forms.⁶⁹ Compared with other bioprinting methods, SLA has the advantages of high precision, fast speed, etc. In the biological field, SLA is often applied to print controllable geometric shapes, including high-precision tissue scaffolds with porous structures.⁷⁰ SLA can achieve higher cell vitality (>85%) without applying shear force to cells and has the ability of fast bioprinting structure with high resolution ($\approx 1\text{ m}$). However, one of the main disadvantages of SLA is that the liquid must be transparent. Otherwise, light would not pass through the material uniformly, resulting in a nonuniform crosslinking. Due to this requirement, the cell density in bioink is limited to about 10^8 cells/ml.⁷¹ In 2014, cell-loaded SLA printing was implemented by the Boland team in Clemson University. Zhu et al.⁷² constructed pre-vascularized tissue with complex 3D microstructure by micro-size continuous optical

bioprinting. At present, SLA technology is widely used in scaffold printing, while it is rarely used in cell-based printing.

Summary and comparison of common skin 3D bioprinting technologies

3D bioprinting technology has the advantages of multi-cell spatial directional manipulation and controllable deposition of different cell densities, which make it the most ideal method for constructing active 3D cell structures in vitro. Different 3D bioprinting technologies have different printing mechanisms, in which the printing equipment, viscosity of the bioink, the concentration and viability of cells, the temperature, and the gelation time of the biomaterials are important factors affecting the bioprinting results. Table 2 summarizes the main parameters of several common different bioprinting technologies. Figure 3 shows the EBB equipment owned by our research group and some scaffolds for pre-printing.

The essential elements for skin bioprinting

The first step of skin 3D bioprinting is to prepare bioink. The second step is to accurately print skin substitutes according to requirements. The printed skin substitutes can be directly transplanted to the wound surface or can be transplanted to the skin wound surface after in vitro culture. The scaffold material is gradually degraded and absorbed in the body, and the implanted cells or bioactive substances continuously proliferate and secrete ECM in the body, eventually replacing the absorbed biological scaffold, completing the regeneration of skin tissue, and achieving skin wound repair.

Bioink plays a key role in skin 3D bioprinting (Figure 4). Bioink refers to biomaterials that have 3D printing ability and can be used to load or wrap living cells or bioactive factors.⁶⁷ During the printing process, the bioink makes direct contact with the cells, maintaining their activity, and provides a supporting microenvironment for maturation of bio-printed skin tissue. Therefore, an ideal bioink should have the following properties: (1) good printing adaptability, (2) high biocompatibility, (3) good mechanical stability, (4) good biodegradability, (5) simulates the in vivo microenvironment of specific cell types, and (6) can support and promote cell activities such as adhesion, migration, proliferation, and differentiation.^{73,74} This section will discuss the applications and limitations of bioink in skin tissue bioprinting, including biomaterials, seed cells, and bioactive factors.

Biomaterials suitable for bioink

At this time, biomaterials that constitute bioink are basically divided into two types: natural biomaterials and synthetic

biomaterials. Natural biomaterials include substances present in ECM, such as collagen, gelatin, fibrin, and hyaluronic acid (HA), as well as other natural biomaterials, such as acellular dermal matrix (ADM), agarose, alginate, chitosan (CS), and silk fibroin. Natural materials have good biocompatibility, but they have the disadvantages of insufficient mechanical properties and long gelation times. Unlike natural biomaterials, synthetic biomaterials have more controllable mechanical and chemical properties. Polyethylene glycol (PEG), polylactic acid (PLA), polycaprolactone (PCL), and gelatin methacrylate (GelMA) are widely used as bioink in 3D bioprinting. However, these materials lack suitable biocompatibility and biodegradability, which limits their application in 3D bioprinting.

Natural biomaterials for skin 3D bioprinting. Collagen, as a natural polymer material, has good biocompatibility, can promote cell adhesion, proliferation, and migration, is safe for the host, does not cause serious inflammation or immune rejection,⁷⁴ and can be enzymatically degraded. It can be printed at a low temperature and forms a solidified gel at body temperature.^{75,76} However, low mechanical strength and slow gelation speed limit the application of collagen.⁷⁷ As a denatured form of collagen, gelatin also has good biocompatibility. Gelatin can be thermally cross-linked to gels, and the gel strength depends on its concentration.^{78,79} HA is an anionic polysaccharide that promotes tissue regeneration, such as cartilage. Due to its poor mechanical properties, it is usually modified with acrylic acid to form a 3D scaffold by photocuring.⁸⁰ Low molecular weight HA can promote cell differentiation and angiogenesis.⁸¹ Agarose is in gel form at room temperature and melts at temperatures above 90°C.²⁰ Agarose printing has the advantages of high mechanical strength without immunogenicity, but has the disadvantage of low cell adhesion.⁸² Alginate is a naturally derived linear polymer from the cell wall of brown algae.⁸³ Alginate printing can retain cell viability and the gelation time is short. In addition, it has outstanding biocompatibility, biodegradability, non-antigenicity, and chelating ability.⁸⁴ The main disadvantages of alginates are their weak mechanical properties, poor cell adhesion, and the lack of alginate-degrading enzymes in mammals.^{85,86} CS is derived from chitin, which is a polysaccharide found in the exoskeleton of shrimp and other sea crustaceans.⁸⁷ CS has a linear structure, which can be quickly formed into a gel matrix using NaOH as a crosslinking agent.⁸⁸ CS has good biocompatibility, biodegradability, and bacteriostatic effect, but its slow gelation speed, low mechanical strength, and fast degradation speed limit its application.^{78,81}

ADM is an emerging material for tissue engineering applications. ADM is produced through a series of physical and chemical treatments to remove all cells and components from the dermis that may be recognized by the host and cause rejection. ADM retains the components and complexity of natural ECM which makes the bio-printed

Table 2. The comparison of the main parameters of several common different bioprinting technologies.

3D Bioprinting technologies	Print speed	Resolution (μm)	Viscosity of bioink (MPas)	Cell concentration	Cell viability	Disadvantages	Advantages	References
Extrusion-based bioprinting	Slow	100–200	$30^{-6} \times 10^7$	High	80%–90%	Lower resolution	Wide range of available materials, printability of highly viscous bioinks, Can print porous structure	Michael et al. ⁵⁸
Laser assisted bioprinting	Medium	pL level	1–300	$\leq 1 \times 10^8/\text{ml}$	>95%	Slow printing speed (limited by gel method), Comparatively high costs	High-resolution, high cell viability (>95%)	Duan et al. ¹⁴ Binder et al. ⁴⁷
Droplet-based bioprinting	Fast	30–60	–	–	70%–90%	The range of available materials is small, Heat and shear can damage cells, and is not suitable for single-channel printing	Low cost and flexible printing process	Fitzpatrick and Morelli ³⁹
Electrostatic inkjet bioprinting	Fast	10–60	–	–	70%	–	Low cost and flexible printing process	Chung et al. ⁴¹
Piezoelectric inkjet bioprinting	Fast	50–100	–	–	70%–90%	Contains glass parts, not suitable for printing certain bioinks, such as fibrinogen	Suitable for single channel printing	Chung et al. ⁴¹
Stereolithography	Fast	High ($\approx 1 \mu\text{m}$)	No limitation	$\leq 1 \times 10^8/\text{ml}$	>85%	Crosslinking requires transparent and photosensitive bioink limiting choice of additives and cell density	High cell viability, High variety of printable bioinks, High resolution of bioprinting	Serra et al. ⁶⁰ Patrascioiu et al. ⁶¹

“–” means no valid data is obtained.

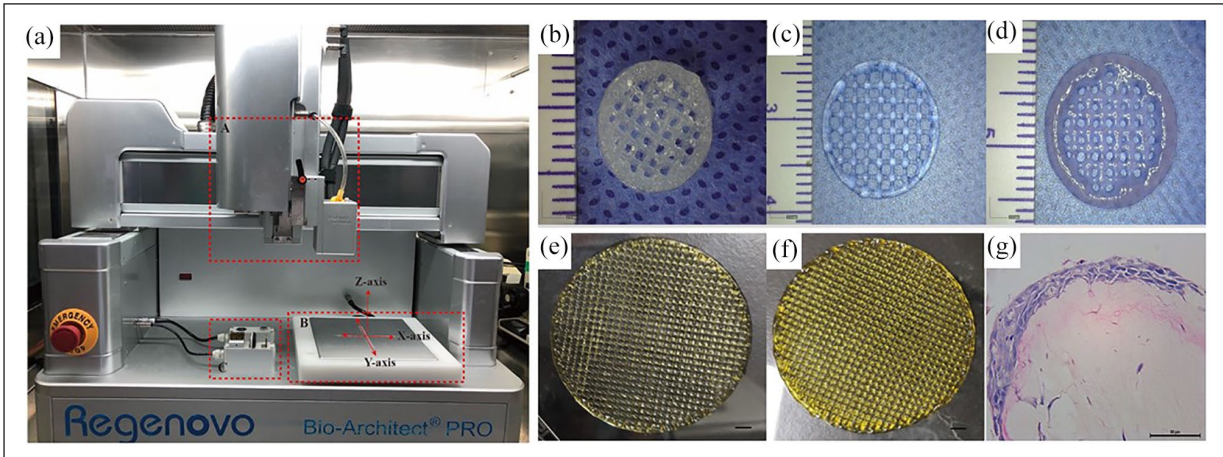


Figure 3. (a) Device diagram of extrusion-based bioprinting. Dotted line frame A is an extrusion device, dotted line frame B is a printing platform, and dotted line frame C is a cleaning and correction device, wherein the cleaning device is located at the front, which mainly cleans syringes, and the rear is a correction device, (b) hydrogel scaffold printed with 1% ADM and 5% GelMA, (c) hydrogel scaffold printed with 2% ADM, (d) hydrogel scaffold printed with 100 ppm AgNPs and 15% GelMA, (e) printed 100 ppm AgNPs and 15% GelMA scaffolds, and (g) HE staining of 3D bioprinted skin after 14 days of gas-liquid culture (b–d: bar:2 mm, E: bar:5 mm, G: bar:50 μ m).

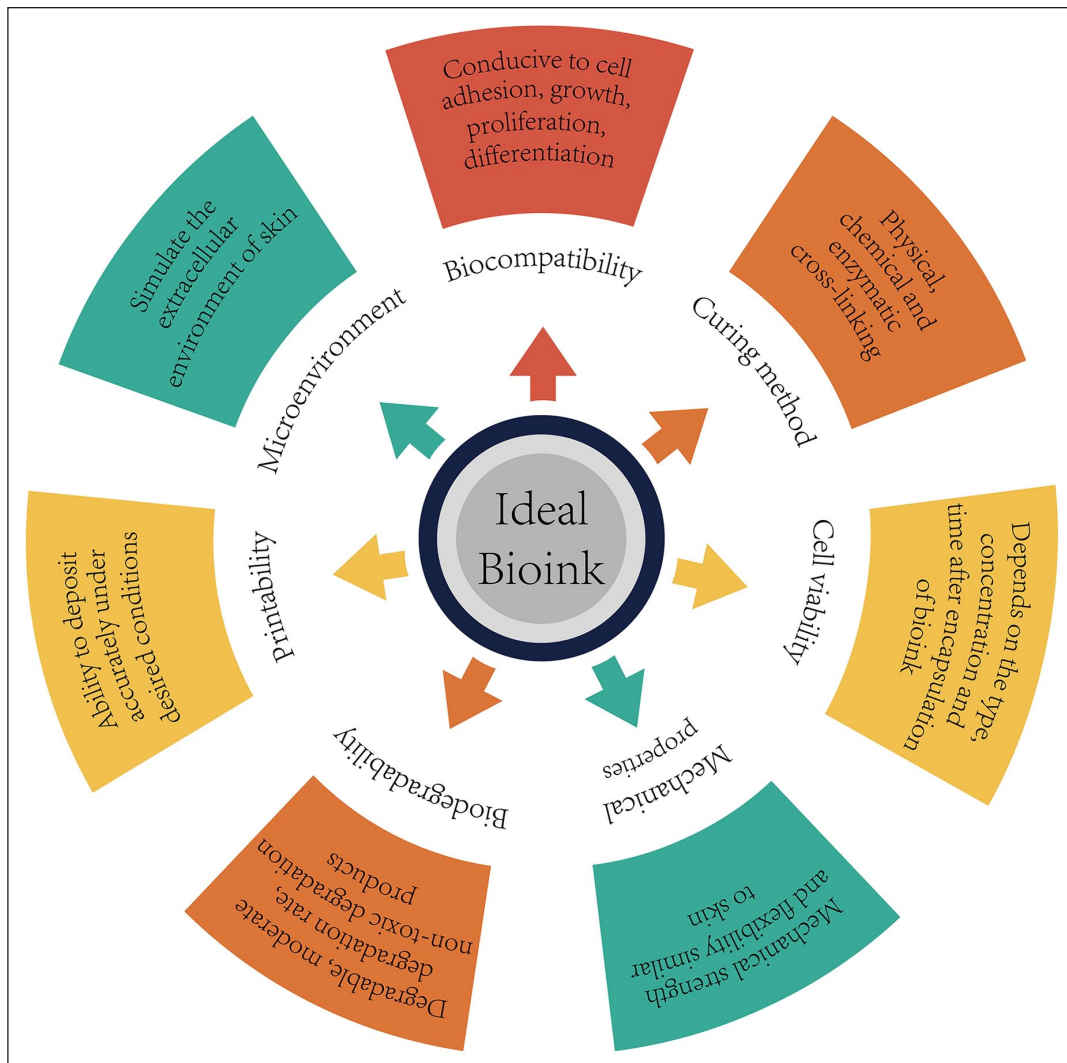


Figure 4. Design strategy of ideal bioink.

ADM structure suitable for reconstructing the microenvironment for printed cells to improve morphology and function.^{89,90} Therefore, ADM has high biocompatibility and low immunogenicity. ADM can gel at 37°C at an appropriate pH.⁹¹ Ventura et al.⁹² proved isopropanol/surfactants could effectively remove cell and lipid during decellularization while preserving the higher amount of ECM proteins. Khan and Bayat⁹³ performed qualitative and quantitative analyses of our decellularized scarred dermis, and these analyses may influence the cellular compartment during cutaneous wound healing. Leng et al.⁹⁴ described a skin scaffold map by integrated proteomics and systematically analyzed the interaction between ECM proteins and epidermal cells in skin microenvironment on this basis. They had revealed that ECM played a role in determining the fate of epidermal stem cells through hemidesmosome components. Some studies have mixed mouse embryo Fbs into porcine ADM for 3D bioprinting and observed that mouse embryo Fb had higher cellular activity on the 7th day of culture.⁹⁵ The skin model using skin ADM provided well-organized/stratified epidermis and stabilized/fibroblasts-stretched dermis during tissue maturation. Possibly, the ECM components such as HA, fibronectin, collagen type I, and other types of collagen might enhance the cellular functionality of ADM.⁹⁶ However, its disadvantages are poor mechanical properties, low printing resolution, and easy collapse when the printing equipment has no heating module.

Composite natural biomaterials are also commonly used in bioprinting. Collagen and alginate are materials commonly used for biological scaffolds.⁹⁷ Previous studies have shown that collagen/alginate scaffolds printed by continuous EBB showed good structural stability and resulted in good cell viability, similar to a pure collagen scaffold. In an *in vivo* test, the collagen/alginate scaffold was used as a dermal substitute and provided good granulation tissue formation and rapid vascularization.⁹⁸ CS can be combined in porous matrices with other natural biomaterials to enhance their properties. Such a combination increases cell proliferation and shows improved cell mobility, migration, and multiplication.⁹⁹ Collagen-CS scaffold (CCS) has the characteristics of appropriate pore size, good biocompatibility, and low antigenicity. It is a proper material for constructing a TE dermal substitute and has great potential in 3D bioprinting applications.^{100,101} However, composite natural biomaterials still have poor mechanical properties, making them susceptible to shrink and deform in the mechanical environment *in vivo*, which makes maintaining the original 3D porous structure difficult, thus limiting the growth of cells, blood vessels, and tissues. Therefore, materials with more controllable mechanical properties are required for 3D bioprinting.

Synthetic biomaterials for skin 3D bioprinting. The mechanical properties and controllability of synthetic biomaterials

exceed those of natural biomaterials.²⁰ Synthetic polymer materials such as PLA, PCL, poly-glycolic acid (PGA), poly lactic-co-glycolic acid (PLGA), as well as GelMA are commonly used for skin bioprinting.¹⁰² PLA has good mechanical and physical properties and biocompatibility and can be completely degraded into carbon dioxide and water in the body.¹⁰³ Therefore, PLA is widely used in the field of biological TE. Using PLA as raw material, TE scaffold can be manufactured by 3D printing technology. The scaffold is beneficial to cell adhesion, differentiation, and growth.¹⁰⁴ Rogina et al.¹⁰⁵ first prepared PLA scaffold by 3D printing and then mixed PLA scaffold material with CS/HA solution to prepare porous composite scaffold using a thermally-induced phase separation method. The results showed that PLA significantly improved the mechanical properties of porous composite scaffold. PLGA is a representative polyester compound and has good mechanical properties and biocompatibility. The degradation rate of PLGA can be modulated by adjusting the ratio of lactic acid to glycolic acid. PLGA is commonly used in the construction of TE scaffolds and bioink.^{106,107} A PLGA mesh/CCS hybrid constructed in our previous report has excellent mechanical properties with an appropriate 3D porous structure.¹⁰⁸ Similarly, PCL is a FDA-approved biodegradable polyester and is amenable to surface modifications, which makes it suitable for tissue repair.¹⁰⁹ PCL nanofiber scaffolds prepared by electrostatic spinning have sufficient mechanical strength to withstand the pressures of cell proliferation and differentiation *in vitro* and *in vivo*.¹¹⁰ The degradation rate of PCL is lower than other materials (such as PGA, PLGA, and Poly L-lactic acid (PLLA))¹¹¹; therefore, PCL nanofibers provide a long-term mechanical support in defective tissue. To reduce excessive scarring in wound healing, Kim et al.¹¹² fabricated electrospun nanofibrous meshes, composed of haloarchaea-produced biodegradable elastomer poly(3-hydroxybutyrate-co-3-hydroxyvalerate) (PHBV) as a wound dressing. And the results demonstrated that electrospun nanofibrous PHBV meshes mitigate excessive scar formation by regulating myofibroblast formation, showing their promise for use as wound dressings. GelMA undergoes photoinitiated radical polymerization (i.e. under UV light exposure with the presence of a photoinitiator) to form covalently crosslinked hydrogels.¹¹³ The polymerization can be performed under mild conditions (neutral pH, aqueous environment, room temperature, etc.) and the reaction can be controlled in time and space.¹¹⁴ This allows for the micromachining of hydrogels to create unique morphologies, patterns, and 3D structures. GelMA with excellent biocompatibility, degradability, and processability will play an important role as a printable biomaterial in 3D bioprinting technology.

Composite biomaterials for skin 3D bioprinting. It is an urgent problem to improve the mechanical properties of materials

based on maintaining good biocompatibility is an important issue. Some studies have indicated that a polymeric blend of PCL/gelatin addressed the shortcomings of natural and synthetic polymers, resulting in a new biomaterial with good biocompatibility and improved mechanical, physical, and chemical properties.^{115–118} Chong et al.¹¹⁶ observed significant cell adhesion, growth, and proliferation of human skin Fbs on electrospun PCL/gelatin scaffolds. To mimic skin ECM hierarchy, Pallabi et al. developed a bilayer 3D structure with varied morphology via electrospin differential stirring periods of a PCL/CS emulsion. The porous structure of the 3D scaffold layer allows for an influx of host cells, integrates effectively with the wound bed, and facilitates the deposition of granulation tissue matrix, while surface exposure of the nanofibrous membrane layer with a limited aperture prevents water loss and serves as the basis for the migration of KCs.¹¹⁹ In addition, enhanced dermal regeneration templates (PLGA knitted mesh-reinforced collagen/CS scaffolds, PLGA/CCS)^{120,121} independently developed by our research group have suitable 3D porous structure, biological properties matching skin tissue, and the ability to rapidly induce tissue regeneration.

Numerous studies have shown that adding natural polymers to GelMA can significantly improve its mechanical properties.¹²² This use of the additive HA with GelMA to produce a GelMA/HA mixture enhanced printability over GelMA alone.¹²³ Stratsteffen et al.¹²⁴ reported that GelMA-collagen hydrogels showed favorable biological and rheological properties, which were suitable for the manufacture of pre-vascularized tissue replacement by 3D bioprinting. Shi et al.¹²⁵ reported a novel bioink made of GelMA and collagen doped with tyrosinase used to 3D bioprint living skin tissues through extrusion bioprinting. Their results showed that bioink can form stable 3D living constructs using the 3D bioprinting. Cell culture studies showed that three major cell lines ([human MCs, human KCs (HaCat), and human dermal Fbs], exhibit high cell viabilities (>90%). In vivo tests have shown that wound healing rates can be accelerated when treated with tyrosinase-doped bioinks.

Seeding cells

Natural skin contains nearly a dozen lineages of differentiated cells and pluripotent stem cells, and various cells are positioned relative to each other with high specificity. At this time, the sources of seed cells for 3D-printed skin are mainly KCs, Fbs, and stem cells including epidermal stem cells (ESCs), adipose-derived stem cells (ADSCs), amniotic fluid-derived stem cells (AFSCs), MSCs, bone marrow MSCs (BMSCs), and induced pluripotent stem cells (iPSCs).

Dermal cells are mainly Fbs, which can secrete collagen and elastin to promote wound healing, and can also

secrete fibroblast growth factor (FGF) to regulate the function of epidermal cells.¹²⁶ Related studies have found that even in the same anatomic location, Fbs are composed of many subgroups with unique phenotypes and functions. Fbs in each subgroup have obvious heterogeneity, and each subgroup affects different stages of wound healing and skin regeneration.^{127–130} CD26 can be used as a new marker to distinguish different Fb subpopulations. Our research group found through previous studies that CD26 could increase collagen deposition in wound tissues, promote the process of wound epithelization and shorten wound healing time by regulating fibroblast proliferation, migration, adhesion, synthesis and secretion of ECM, and other biological behaviors. Therefore, we speculate that adding CD26⁺ Fbs as seed cells to dermal printing is expected to accelerate wound healing. KCs are the principal cells of the epidermis. During the process of keratinization, they migrate up from the basement membrane toward the stratum corneum. KCs can synthesize keratin¹³¹ and have the capacity to increase their rate of replication during periods of inflammation, disease, or injury.¹³² Electrospun nanofiber scaffolds seeded with skin cells (e.g. dermal Fbs and KCs) have been applied for full-thickness wound repair.¹³³ Sheikh et al.¹³⁴ reported a cold plate electrospinning technique for manufacturing 3D nanofiber structures that were co-cultured with human skin Fbs and KCs to make skin substitutes. In another study, Wang et al. created a skin tissue construct with electrospun PCL/collagen nanofibers and Fbs and KCs. After 2 weeks of culture in vitro, the construct was implanted into full-thickness wounds in nude mice, which resulted in an effective healing of these wounds with complete wound closure and epidermal regeneration.¹³⁵ In summary, KCs and Fb are often used as skin seed cells in 3D bioprinting technology.

Ideally, 3D bioprinted skin should have various functions that include functional blood vessels, normal pigmentation, and various skin appendages (hair follicles, sweat glands, sebaceous glands). Since angiogenesis is an important factor that determines the success of 3D printed skin, endothelial cells have been used along with other cells during printing.^{77,136,137} Normal skin pigmentation is formed by the transfer of melanin from MCs to surrounding KCs. At this time, some scientists have already constructed TES that exhibits pigment function through incorporation of MCs.¹³⁸ Another studies have shown that MCs in the epidermis may originate from MC stem cells in the bulge of the hair follicle.¹³⁹ Therefore, MCs, MC stem cells, and KCs are expected to become seed cells for 3D skin printing to solve the skin color problem. Recent studies have shown that hair follicle stem cells (HFSCs) and hair papilla cells (HPCs), as hair follicle seed cells, play an important role in the formation and regeneration of hair follicles. HFSCs include hair follicle epidermal stem cells (HFESCs) and hair follicle dermal stem cells (HFDESCs).

HFESCs have the potential to regenerate the skin and can form epidermal structures. HFESCs can form skin appendages such as hair follicles, sweat glands, and sebaceous glands under the appropriate microenvironment.¹⁴⁰ There are relatively few studies on HFDESCs, and it is currently believed that HFDESCs may be located in the dermal sheath of the hair follicle. HFDESCs, as “reserve cells” or precursor cells of hair papillae, play an important role in maintaining a constant number of HPCs. HPCs controls the signals of hair follicle growth and cycle and plays a key role in the process of hair follicle regeneration. Studies have confirmed that HPCs have specific “aggregation” growth characteristics and have the functions of inducing hair follicle regeneration and supporting hair growth *in vivo* and *in vitro*.¹⁴¹ In terms of skin sweat gland reconstruction, the stem cells used for sweat gland regeneration mainly include ESCs, MSCs, BMSCs, and mammary progenitor cells (MPCs).

Most current TE strategies depend on a sample of autologous cells from the damaged host tissue or organ. When it is difficult to obtain cells from the damaged host, especially when the injury or damage is extensive, alternative cell sources become a necessity. In recent years, with the development of stem cell technology, more stem cell types have been applied to 3D skin printing. ADSCs can be applied in skin 3D bioprinting. Due to the popularity of plastic liposuction, ADSCs are readily available in large quantities and can be applied to 3D bioprinting without amplification. ADSCs can secrete a variety of cytokines to promote Fb migration during wound healing. They can also upregulate the expression of vascular endothelial growth factor (VEGF) and promote neovascularization.¹⁴² MSCs have therapeutic potential for repair and regeneration of tissues damaged by injury or disease. MSC treatment of acute and chronic wounds results in accelerated wound closure, increased epithelialization, formation of granulation tissue, and angiogenesis.¹⁴³ Many clinical trials have demonstrated that BMSCs play a critical role in wound repair and tissue regeneration. Therefore, they are an ideal cell source for skin and appendage regeneration.¹⁴⁴ AFSCs are an attractive cell source for regenerative medicine because of their high proliferation capacity, multipotency, immunomodulatory activity, and lack of significant immunogenicity.^{144,145} Unlike embryonic stem cells, AFSCs do not form teratomas when injected into immunodeficient mice. Furthermore, the isolation of AFSCs is a simpler process than that of MSCs, and a large number of AFS cells can be isolated and expanded from as little as 2 ml of amniotic fluid.^{145,146} iPSCs have multi-directional differentiation potential and can differentiate into all cells derived from three germ layers *in vivo*, making them a good choice for seed cells for disease treatment. Studies showed that iPSCs could differentiated into various types of skin cells with the capacity to form multi-differentiated epidermis with hair follicles and sebaceous glands.¹⁴⁷ Previous studies have developed skin constructs using

iPSC-derived Fbs, KCs, and MCs.¹³⁶ Therefore, it is possible to regenerate skin and skin appendages with iPSC cells.¹⁴⁸ Stem cells have shown potential in the field of TES, but the specific mechanism by which stem cells play a role in wound healing is unclear and it is difficult to avoid potential risks such as mutations and tumorigenicity during the culture process. The ethical challenges around stem cells persist across various fields.

Bioactive factors

At this time, growth factors applied to bio-printed skin include epidermal growth factor (EGF), FGF, VEGF, or platelet-derived growth factor (PDGF). The effects of adding growth factors in the process of 3D skin printing include stimulating growth, proliferation, and migration of various cells, improving the activity of cells in printed skin, inducing the differentiation of stem cells to a preset direction, and driving autologous endogenous cells to gather around the wound when applied *in vivo*. EGF, a single polypeptide chain of 53 amino acids with three interchain disulphide bonds required for biological activity,¹⁴⁹ plays an important role in accelerating and enhancing wound healing by stimulating proliferation of most epithelial cells, Fbs, endothelial cells, and even collagen deposition.^{150,151} It also stimulates the migration and proliferation of KCs.¹⁵² Huang et al.⁷⁹ created a cell-laden 3D-ECM. The bioprinted 3D-ECM mimicked organized patterns of mouse plantar dermis components, and EGF within composite gelatin and sodium alginate hydrogels yielded important information for the effective and accurate differentiation of mouse dorsal epithelial progenitors *in vitro* and *in vivo*. FGF-2 is a multifunctional poly-peptide that promotes growth, migration, and differentiation of a broad variety of cell types, including dermal Fbs, KCs, endothelial cells, and MCs.¹⁵³ FGF-2 is known to stimulate VEGF expression, granulation tissue formation, and blood vessel maturation.^{154–156} Xiong et al.¹⁵⁶ added FGF-2 to a 3D-printed gelatin-fibroin scaffold. The results showed that the incorporation of FGF-2 into the scaffold increased the cell proliferation rate (about 40%–75%) and promoted the healing of full-thickness skin defects. One of the major limitations of skin bioprinting, as is true for engineering most tissue types, is achieving vascularity.¹⁵⁷ Early attempts applied growth factors such as VEGF¹⁵⁸ with KCs or scaffolds such as gelatine-sulfonated silk composite to encourage neovascularization.¹⁵⁶ Recent studies had found that the pro-angiogenic secretome from human skin-derived multipotent stromal cells had the potential to promote skin regeneration.¹⁵⁹ In future studies, growth factors can be added to bioprinted skin. These factors can increase the activity of cells, facilitate the survival of artificial skin, and accelerate wound healing. On the other hand, with the enhancement of cell proliferation activity, the biocompatibility requirements of bioink materials can be relatively reduced, so the selection range of materials will be further expanded.

The development of bioink is a major challenge. Firstly, bioink should have excellent biocompatibility. Only by forming a microenvironment similar to the ECM can further regulate the cell behavior after printing and construct the communication and connection between cells. Due to the special process of the 3D bioprinting, the bioink is required to exist in a dynamic state during printing, and then can be solidified and formed rapidly after printing. Therefore, printability is another requirement that bioink needs to meet. Shape fidelity, gelation kinetics, rheological characteristics, material properties, and printing resolution are important considerations when assessing the printability of bioink.¹⁶⁰ Similarly, the biomechanical and structural characteristics of the skin are also important considerations for choice of bioink. The ideal skin printable bioink should be able to support the functions of different types of cells in the skin and promote the regeneration of skin appendages and angiogenesis. In summary, the development of skin printing bioink with suitable physical and chemical properties is still a key core issue in skin 3D bioprinting.

Regeneration of skin tissue and appendages through 3D bioprinting

In this section, we present the current research status and progress of 3D bioprinted full-thickness skin, dermis, skin vascularization, skin pigmentation, and skin appendages including sweat glands and hair follicles, and discuss future development direction and clinical applications (Table 3).

Dermis bioprinting

The integrity of the dermal structure is closely related to the elasticity and flexibility of the skin. Reconstruction of the integrity and continuity of dermal tissue structure through 3D bioprinting technology has made important progress in effectively repairing wounds. Ng et al.¹⁶¹ reported the use of polyelectrolyte gelatin-CS (PGC) hydrogel for 3D bioprinting of dermis. The inherent antimicrobial and hemostatic properties of CS make it compatible in wound healing applications. The PGC hydrogels showed good printability at room temperature, high shape fidelity of the printed 3D constructs, and good biocompatibility with Fbs. Michael et al.⁵⁸ used a laser-assisted bioprinting technique to create dermal substitutes. They positioned Fbs on top of a stabilizing matrix (Matriderm). Subsequently, the grafts were placed into full-thickness skin wounds in nude mice. The grafts adhered well to tissue around the skin wound after 11 days. Some blood vessels were found to grow from the wound bed and the wound edges in the direction of the printed cells. Furthermore, normal skin grew into the printed dermis layer, and the upper layer of dermis collagen was dense

while the lower layer was sparse, which conformed to the normal dermal structure of the human body.

Bioprinting of full-layered skin

At present, the number of cases of skin defects caused by trauma, burns, ulcers, and surgical trauma is increasing. The introduction of 3D-bioprinted skin makes it possible to customize autologous skin for patient wounds or to directly perform in situ skin bioprinting to treat wounds. Previous studies have shown that 3D-printed skin is similar to normal skin tissue when mature. Lee et al.¹⁶² used KCs and Fbs as seed cells to print skin tissue. Collagen was used to function as the dermal matrix of the skin. Optimizing printing parameters for maximum cell viability and cell densities in the epidermis and dermis is important to mimic physiologically relevant attributes of human skin. Histology and immunofluorescence showed that 3D-printed skin tissue was morphologically and biologically representative of in vivo human skin tissue. Cubo et al.¹⁶³ used a 3D bioprinting technique (free-form fabrication bioprinting.) to print a human bilayered skin using bioinks containing human plasma and primary human Fbs and KCs that were obtained from skin biopsies (Figure 5). Based on careful histological and immunohistochemical in vitro and in vivo analysis, they demonstrated that the printed skin was very similar to normal human skin. To overcome poor printability and long cross-linking duration of collagen biomaterials, Wang et al.¹⁶⁴ designed and printed a bilayer membrane (BLM) scaffold consisting of an outer PLGA membrane and a lower alginate hydrogel layer, which mimicked the skin epidermis and dermis, respectively. The multi-porous alginate hydrogel of the BLM scaffolds promoted cell adhesion and proliferation in vitro, while the PLGA membrane prevented bacterial invasion and maintained the moisture content of the hydrogel. The results showed that the application of a BLM scaffold resulted in high levels of skin regeneration by increasing neovascularization and boosting collagen I/III deposition. Lee et al.¹⁶⁵ used a solid freeform fabrication (modified version of extrusion-based bioprinting) technique to create multi-layered engineered tissue composites. Collagen-based hydrogel bioink was printed in a layer-by-layer fashion, resulting in two distinct cell layers of inner Fbs and outer KCs. Highly viable proliferation of each cell layer was observed on both planar and non-planar surfaces.

In situ bioprinting involves direct printing of pre-cultured cells onto the site of injury for wound closure, allowing for skin maturation at the wound site. The application of in situ bioprinting in burn wound reconstruction provides many advantages, including accurate deposition of cells on the wound, elimination of the need for expensive and time-consuming in vitro differentiation, and the need for multiple surgeries.¹⁶⁶ Binder¹⁶⁷ used inkjet bioprinting

Table 3. Examples of bioprinted skin tissues.

Skin tissues	Cell sources	Materials	Printing method	Results	References
Dermis	Neonatal human foreskin Fbs NIH3T3 Fbs	Polyelectrolyte gelatin-chitosan hydrogel Matriderm®	DOD bioprinting Laser-assisted	The printed 3D constructs showed high shape fidelity and good biocompatibility with fibroblasts. The printed fibroblasts produced collagen, some blood vessels were found to grow in the direction of the printed cells.	Ozolat and Hospodiuk ⁴⁸ Maxson et al. ¹⁴³
Full-layered skin	Primary human Fbs and KCs Primary human Fbs and KCs Human KCs and Fbs Allogeneic or autologous dermal Fbs and epidermal KCs	Collagen hydrogel Human plasma Fibrinogen/collagen hydrogels Fibrin/collagen hydrogel	Extrusion Extrusion Inkjet In situ bioprinting	The stratified layers of printed FB and KC within the multi-layered collagen scaffold were observed. The printed skin was very similar to normal human skin. After 8 weeks, wound healing and complete re-epithelialization were observed. In a murine full-thickness wound model, this in situ bioprinting system showed accelerated wound closure (<15% of original wound size at 2 weeks) with entire wound closure after 3 weeks post-surgery. Neovascularization was observed in the skin grafts 2 weeks after surgery.	De Coppi et al. ¹⁴⁵ Aasen et al. ¹⁴⁷ Laato et al. ¹⁴⁹ Gainza et al. ¹⁵⁰
Blood vessel-containing skin	Newborn dermis Fbs, KCs, and HUVECs hMSCs and endothelial cells AFSCs and BMSCs Human endothelial cell, and hMSC	Type collagen I and fibrinogen Collagen hydrogel containing VEGF Fibrin-collagen gel Biodegradable PLA fibers and GelMA hydrogels.	Inkjet Laser-assisted A bioprinting device developed in-house FDM 3D bioprinting and SLA bioprinting	Highly organized vascular networks were generated in the construct. Reporting a new approach for creating vascularized, heterogeneous tissue constructs on demand based on 3D bioprinting. Formation of capillary-like structures was dependent on a sufficient local density of endothelial cells. AFSCs and BMSCs can accelerate wound healing and increased microvessel density and capillary diameters.	Fielding et al. ⁶⁵ Pal et al. ¹¹⁹ Zuo et al. ¹²⁹ Duncan et al. ¹⁵⁸
Melanocytes-containing skin	HUVECs and Fbs HUVECs, Fbs, KCs MCs, Fbs, and KCs (HaCaT) KCs, MCs, and Fbs from three different skin donors	Pluronic F127 and GelMA Acellular fat matrix and fibrinogen as the subdermal layer; Gelatin and thrombin were used as vascular channels. ADM was used as a dermis layer Multiple layers of collagen hydrogel Hierarchical porous collagen-based structures	3D bioprinting Extrusion and inkjet Extrusion A two-step DOD bioprinting	A novel printing platform is suggested for engineering a matured perfusable vascularized 3D human skin equivalent composed of epidermis, dermis, and hypodermis. MC-containing epidermal layer showed freckle-like pigmentations at the dermal-epidermal junction. Histological analysis indicated the presence of a well-developed epidermal region and uniform distribution of melanin granules in the epidermal region of the 3D-bioprinted pigmented skin constructs.	Ng et al. ¹⁶¹ Cubo et al. ¹⁶³ Wang et al. ¹⁶⁴ Lee et al. ¹⁶⁵ Ozolat ¹⁶⁶
Hair follicle Sweat glands	Dermal papilla cells (DPCs) Mouse dorsal epithelial progenitors; plantar dermis homogenate, and EGF MSCs Mouse mammary progenitor cells (MPCs)	Collagen gel containing dermal fibroblasts A cell-laden 3D extracellular matrix mimics (3D-ECM) with composite hydrogels based on gelatin and sodium alginate Alginate/gelatin hydrogel Gelatin-alginate hydrogels and components from mouse sweat gland extracellular matrix proteins	Extrusion Extrusion Extrusion Extrusion	DPCs in a physiologically relevant extracellular matrix and initiation of epidermal-mesenchymal interactions, which results in HF formation in human skin constructs in vitro. Bioprinted 3D-ECM could effectively create a restrictive niche for epidermal progenitors that ensures unilateral differentiation into sweat gland cells. Representing a novel strategy of directing MSC differentiation for functional SG regeneration by using 3D bioprinting. Differentiated mouse MPCs could regenerate SG cells by engineered SG microenvironment in vitro and Shh pathway was found to be correlated with the changes in the differentiation.	Kang et al. ¹⁷³ Abaci et al. ¹³⁶ Ng et al. ¹⁸⁵ Feng ¹⁹⁴

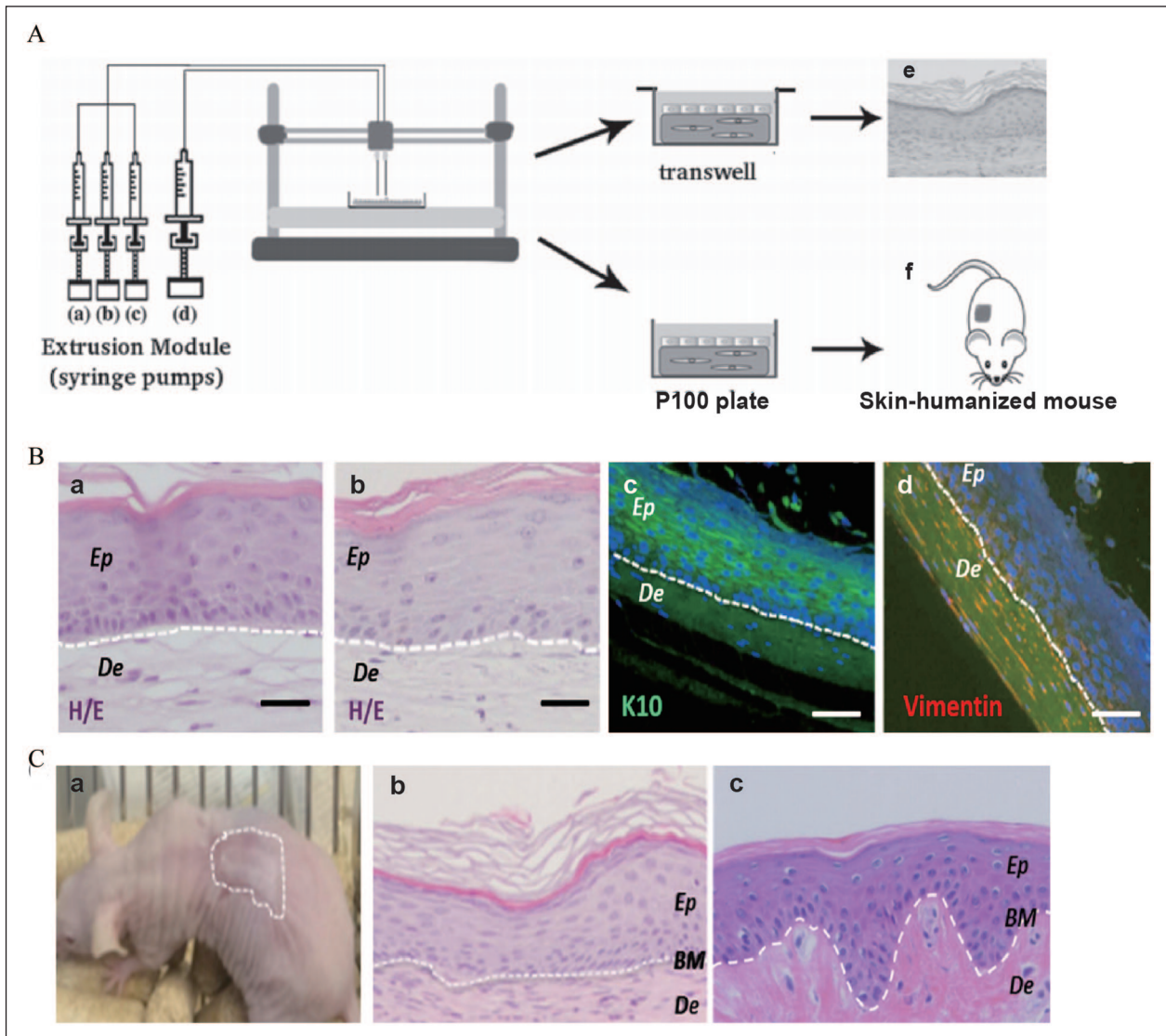


Figure 5. (A) Scheme of the bioprinting process: The extrusion module contained four syringes, loaded with (a) hFbs, (b) plasma, (c) CaCl_2 , (d) hKCs, respectively, (e) equivalents printed on transwell inserts could differentiate at the air-liquid surface for 17 days, and (f) equivalents printed on P100 plates were grafted on to the backs of immunodeficient mice for 8 weeks. (B) In vitro 3D human skin equivalents obtained after 17 days of differentiation at the air-liquid interface: (a) “handmade” skin equivalent following our previous protocol, (b–d) printed skin equivalents, (a and b) H/E staining, (c and d) immunostaining using an anti-K10 antibody (c) and an anti-human vimentin antibody (d). Ep and De in (a–d) denote the epidermal and the dermal compartments, respectively. (C) Histological analysis (8 weeks postgrafting) of bioprinted human skin grafted to immunodeficient mice: (a) visual appearance of the grafted human skin, (b) H/E staining of the regenerated human skin, (c) H/E staining of normal human skin. The white dotted line in (b) and (c) indicates the dermo-epidermal junction (basal membrane, BM). Scale bar: 100 μm .

Source: Adapted with permission from Cubo et al.¹⁶³

technology to directly print primary human KCs and Fbs on full-thickness ($3.0 \times 2.5 \text{ cm}$) wounds on the backs of nude mice. First, Fbs ($1.0 \times 10^5 \text{ cells/cm}^2$) incorporated into fibrinogen/collagen hydrogels were printed on the wounds, followed by a layer of KCs ($1.0 \times 10^7 \text{ cells/cm}^2$) above the fibroblast layer. After 8 weeks, wound healing and complete re-epithelialization were observed. Recently, Albanna et al.¹⁶⁸ developed a portable, easy-to-operate, and relatively inexpensive skin in situ bioprinting system.

First, the entire wound was scanned continuously using a 3D laser scanner, after which the scanned data were converted into a wound model. Using fibrin/collagen as a hydrogel carrier, allogeneic or autologous dermal Fbs and epidermal KCs were directly transported to the whole skin defect to form a layered skin structure. In a murine full-thickness wound model, this in situ bioprinting system showed accelerated wound closure (<15% of original wound size at 2 weeks) with entire wound closure after

3 weeks post-surgery. The dermis structure and composition of regenerated tissue were similar to healthy skin and many collagen deposits were arranged in regular fibers with the formation of mature blood vessels.

The above studies have preliminarily supported the feasibility of 3D bioprinting to construct TES, which has provided a foundation for clinical applications. In addition to wound treatment, 3D-bioprinted skin can also be used as an *in vitro* model for cosmetics and chemical tests. At this time, the European Union has issued a decree banning the testing of cosmetic ingredients on animals. To this end, L'Oreal has developed a patented skin called Episkin for the testing and development of products,¹⁶⁹ which addresses the ethical problems of animal experiments. In addition, 3D bioprinting can generate skin disease models for pathophysiological research, drug screening, or evaluation of therapeutic effects *in vitro*.^{163,170}

Bioprinting of blood vessel-containing skin

Timely vascularization after 3D-printed skin transplantation is key for survival of the graft. Studies have shown that in the absence of blood vessel distribution, the maximum nutrient diffusion distance that can guarantee cell survival is 100–200 μm .¹⁷¹ Thus, tissue constructs with a thickness greater than 100–200 μm require blood vessel distribution. At this time, there are many pro-vascularization methods used in TES, including optimizing the porous structure of TES,^{172,173} loading pro-angiogenic factors, inoculation with vascular endothelial cells,⁷⁷ and stem cells.^{146,174}

To improve the vascularization of printed skin tissues, Yanez et al.⁷⁷ used inkjet printing technology to construct artificial skin with newborn dermis Fb, KC, and human umbilical vascular endothelial cells (HUVECs) as seed cells and type I collagen and fibrinogen as a matrix. 3D-printed skin graft was transplanted into the back wound of thymus-free nude mice. The results showed that 3D-printed skin grafts can accelerate wound healing, and neovascularization was observed in the skin grafts 2 weeks after surgery. Among the above cell types, HUVECs play an important role. Abaci et al.¹³⁶ established a novel bioengineering approach to micropattern spatially-controlled and perfusable vascular networks in 3D human skin equivalents using both primary and iPSC-derived endothelial cells. Using 3D printing technology allows us to control the geometry of the micropatterned vascular networks. These results showed that vascularized human skin equivalents (vHSEs) can both promote and guide neovascularization during wound healing (Figure 6). Kerouedan et al.¹³⁷ developed LAB to pattern lines of tdTomato-labeled endothelial cells cocultured with MSCs seeded onto a collagen hydrogel. Overlay of the pattern with collagen I hydrogel containing VEGF allowed capillary-like structure formation and preservation of the printed pattern

over time. In addition, the use of biomaterials such as fibrin and HA can also promote angiogenesis so that 3D-printed skin can initially provide vascular networks through the printed channels and induce blood vessels to form a replacement for the original hollow network.¹⁷⁵

Previous reports have suggested that the provision of angiogenic growth factors regulates several stages of angiogenesis including endothelial cell migration, vessel sprouting, perivascular cell recruitment, and ECM production.^{176,177} The combination of 3D-printed scaffolds and angiogenic growth factors can significantly improve the vascularization of 3D-printed skin tissue. Xiong et al.¹⁵⁶ demonstrated that 3D-printed gelatin-based silk fibroin scaffolds promoted healing of full-thickness skin defects. Modified silk fibroin with sulphonated moieties was used in the scaffold to increase hydrophilicity, as well as to facilitate incorporation of FGF-2 to further enhance the treatment efficacy. Incorporation of FGF-2 within the scaffold enhanced the proliferation rate (from ~40% to ~75%), tissue morphology, collagen fibril assembly, blood vessel formation, and expression of various corresponding markers. Skardal et al.¹⁴⁶ resuspended AFSCs and BMSCs in fibrin-collagen gel and printed over the full-thickness skin wounds in nude mice. Their results suggested that AFSCs and BMSCs can accelerate wound healing. In addition, histological examination showed increased microvessel density and capillary diameters in the AFSC-treated wounds. Cui et al. explored the fabrication of complex vascularized skin constructs. The construct was fabricated on a dual 3D bioprinting platform comprised of an FDM 3D bioprinter and an SLA 3D bioprinter, using alternate deposition of biodegradable PLA fibers and cell-laden GelMA hydrogels. Moreover, bioactive factors such as bone morphogenetic protein2 (BMP2) and VEGF were incorporated into the construct to simultaneously promote cell proliferation and angiogenesis through the construct. After perfusion culture, highly organized vascular networks were generated.¹⁷⁸

Flow shear stress can promote angiogenesis; thus, dynamic flow is key to develop the vascular system required for full-thickness skin tissue. Mori et al.¹⁷⁹ prepared a perfusable vascular channel in the skin substitute and coated endothelial cells in the channel and then fixed it to a culture device connected to an external pump and tubes. Results showed that vascular channels were constructed in the skin substitute, and the endothelial cells formed tight junctions on the vascular channel wall. The barrier function of the skin-equivalent was also confirmed. To reduce the diameter of vascular channels, some studies have used sacrificial materials. Kolesky et al.¹⁸⁰ used an aqueous fugitive bioink composed of Pluronic F127 to print channels with a pore diameter of less than 45 μm . The remaining structure of the outer ring was printed with GelMA loaded with Fbs, after which the entire structure was cooled to 4°C to liquefy Pluronic F127. Subsequently,

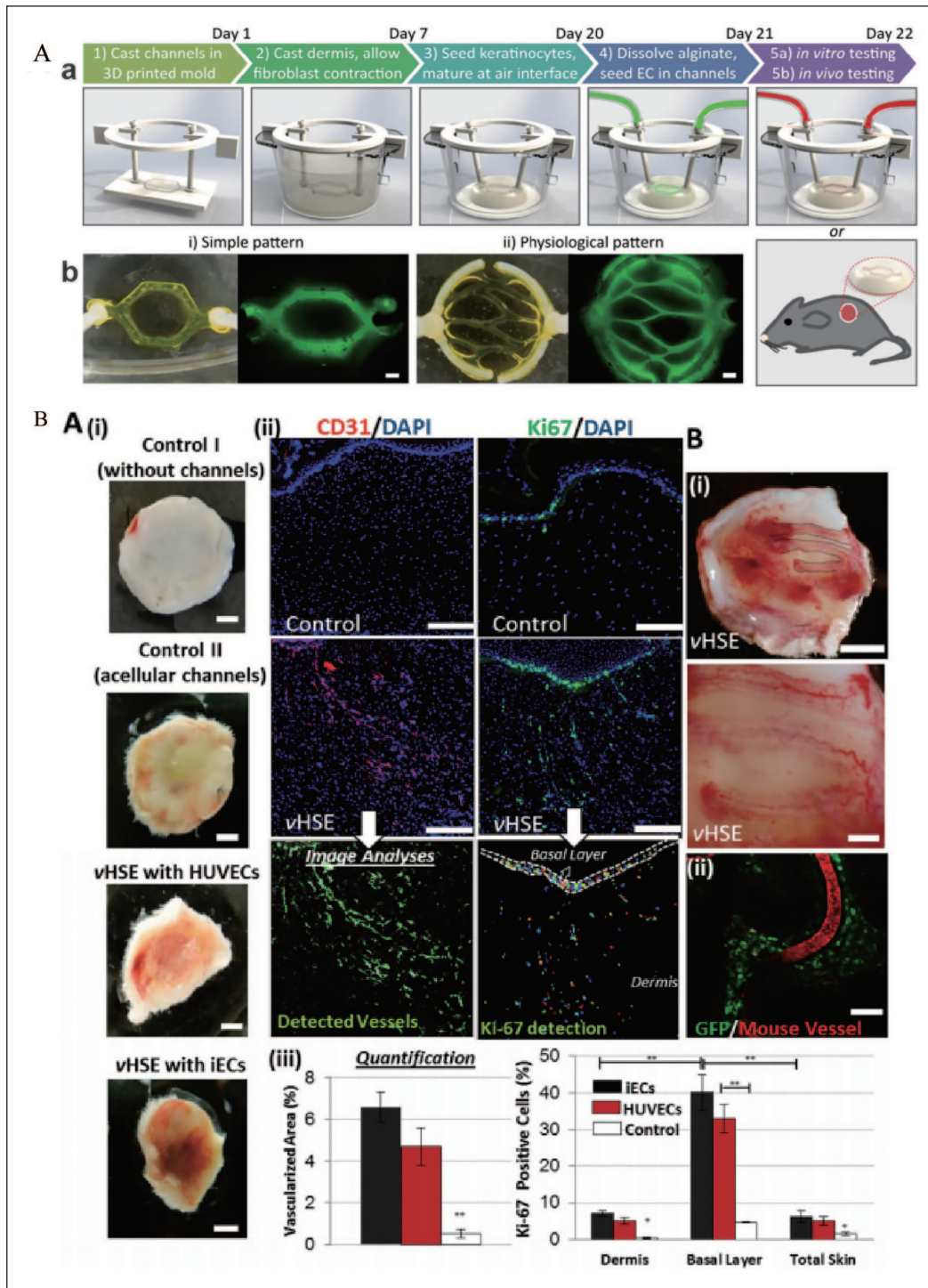


Figure 6. (A) Development of vascularized HSEs: (a) schematic description of the protocol to develop vHSEs, (b) two different vasculature patterns were used in our studies and generated using fluorescently tagged alginate. Scale bar: 600 μ m. (B-a) The effect of vHSEs on host neovascularization. Blood perfusion in HSEs: (i) without channels (Control I), with acellular microchannels (Control II), vHSEs with HUVECs, and iECs grafted on SCID mice and harvested after 2 weeks. Scale bar: 2.5 mm, (ii) immunostaining of explanted HSEs (control) and vHSEs with CD31 (red) and Ki67 (green) to visualize the invasion of the host vessels and the presence of proliferating cells, respectively. Scale bars: 250 μ m, (iii) quantification of the percentage of the total area covered by the host vasculature and the percentage of Ki-67 positive cells (* p < 0.05, ** p < 0.005, and N = 4). (B-b) (i) Pictures of newly formed host vasculature following the micropatterned human iEC-containing microchannels in vHSEs Scale bars: 2.5 mm and 500 μ m, (ii) confocal image of the explanted vHSEs showing the overlapping pattern of Rhodamine-dextran (70 kDa) perfused mice vessels and the microchannels containing GFP-tagged HUVECs (N = 4 for all conditions) Scale bar: 500 μ m. Source: Adapted with permission from Abaci et al.¹³⁶

an empty syringe was used to extract the liquefied Pluronic F127 in the channel, and HUVECs were injected into the channel to achieve endothelialization of the vessel. In addition to using sacrificial materials, Bertassoni et al.¹⁸¹ reported a 3D micromolding technique using bioprinted agarose template fibers to fabricate microchannel networks with various architectural features within photocrosslinkable hydrogel constructs. This method casted GelMA around the printed agarose fibers and then removed the agarose by manual suction instead of using sacrificial materials. In the resulting lumen, HUVECs were used to form a vascular endothelial monolayer structure. Kim et al.^{182,183} developed a fully perfused vascularized 3D-printed skin model. In the self-made PCL transwell chamber, they used acellular fat matrix and fibrinogen as the subdermal layer by extrusion bioprinting. Gelatin and thrombin (sacrificial material) loaded with HUVECs were used as vascular channels. ADM mixed with Fbs was used as a dermis layer and KCs were inkjet printed on the scaffold. The skin model showed good biological characteristics. After 7 days of culture, it was found that the dermis and the subdermal layer were connected, as opposed to the skin model without vascular channels, and formed a stabilized fibroblast-stretched dermis and stratified epidermis layers after 14 days.

Bioprinting of MC-containing skin

One of the main goals of skin 3D bioprinting is to print skin tissues with skin pigmentation function to meet the requirement of patients for normal skin color. Previous studies have successfully printed a full-layer skin model containing pigment using 3D biological printing technology. Min et al.¹⁸⁴ have reported a 3D bioprinting technique that is capable of producing a full-thickness skin model containing pigmentation. Multiple layers of fibroblast-containing collagen hydrogel precursor were printed and crosslinked through neutralization using sodium bicarbonate, constituting the dermal layer. MCs and KCs were sequentially printed on top of the dermal layer to induce skin pigmentation upon subsequent air-liquid interface culture. Results showed MC-containing epidermal layer showed freckle-like pigmentations at the dermal-epidermal junction. Ng et al.¹⁸⁵ demonstrated the feasibility of applying a two-step bioprinting-based strategy to fabricate 3D in vitro pigmented human skin constructs (using KCs, MCs, and Fbs from three different skin donors) (Figure 7). A two-step DOD bioprinting strategy facilitated the deposition of cell droplets to emulate the epidermal melanin units and manipulation of the microenvironment to fabricate 3D biomimetic hierarchical porous structures found in native skin tissue. Histological analysis indicated the presence of a well-developed epidermal region and uniform distribution of melanin granules in the epidermal region of the

3D-bioprinted pigmented skin constructs. Furthermore, immunochemical analysis revealed the presence of important biomarkers (col VII, HMB-45, K1, and K6) in the 3D-bioprinted pigmented skin constructs. The above studies have supported the operability of printing MCs to increase skin pigmentation. However, there are many unanswered questions in these studies, such as whether MCs proliferate after printing and whether melanin has spread to the surrounding KCs. In addition, it remains unclear whether MCs containing melanin stem cells improve the long-term sustainability of pigment formation after 3D-printed skin transplantation.

Bioprinting of hair follicles

Hair follicle reconstruction is the premise for constructing tissue-engineered skin with hair formation ability, and the key to hair follicle reconstruction is to find or improve the ability of seed cells to induce hair formation. Currently, hair follicle seed cells with the best potential are HFSCs and HPCs. The location of these two cells in hair follicles is relatively clear and the isolation method is mature. Studies have shown that newly isolated HFSCs mixed with dermal cells or HPCs mixed with epidermal cells can induce hair follicle regeneration. Wu et al.¹⁸⁶ mixed dermal papilla cells (DPCs), hair follicle epithelial cells, dermal sheath cells, and collagen to form dermal analogues, and then transplanted them under subcutaneous tissue of the dorsal skin of nude mice and the formation of hair fibers was observed. The latest research had found that epidermal CD34⁺ stem cells located in the bulge area of hair follicles can induce HF neogenesis and promote wound healing after transplantation.¹⁸⁷

A prerequisite for hair follicle regeneration in clinical treatment is that the cells must be of ethnic origin. However, most of the HPCs studied for hair follicle regeneration are of mouse origin. Few studies have shown that human HPCs cultured in vitro can regenerate intact hair follicles because human HPCs quickly lose their induction ability in vitro.¹⁸⁸ In a previous study, mouse tissue DPCs and human KCs were used to inoculate TES formed using collagen glycosaminoglycan matrix. Transplantation into nude mice resulted in the formation of new hair follicles; however, hair follicles did not form when human DPCs were used instead of murine DPCs.¹⁸⁹ Therefore, maintaining the induction ability of dermal papilla in vitro remains challenging. The induction of HPCs to hair follicles and the expression of characteristic genes of dermal papilla are highly dependent on their internal microenvironment. After in vitro culture, the expression of many characteristic genes of HPCs, such as Akp2, Alx3, and Alx4, decreased rapidly, accompanied by a decline in hair follicle induction ability. In summary, the greatest challenge in hair follicle regeneration is improving conditions of in vitro 3D culture, which in turn would simulate the growth environment

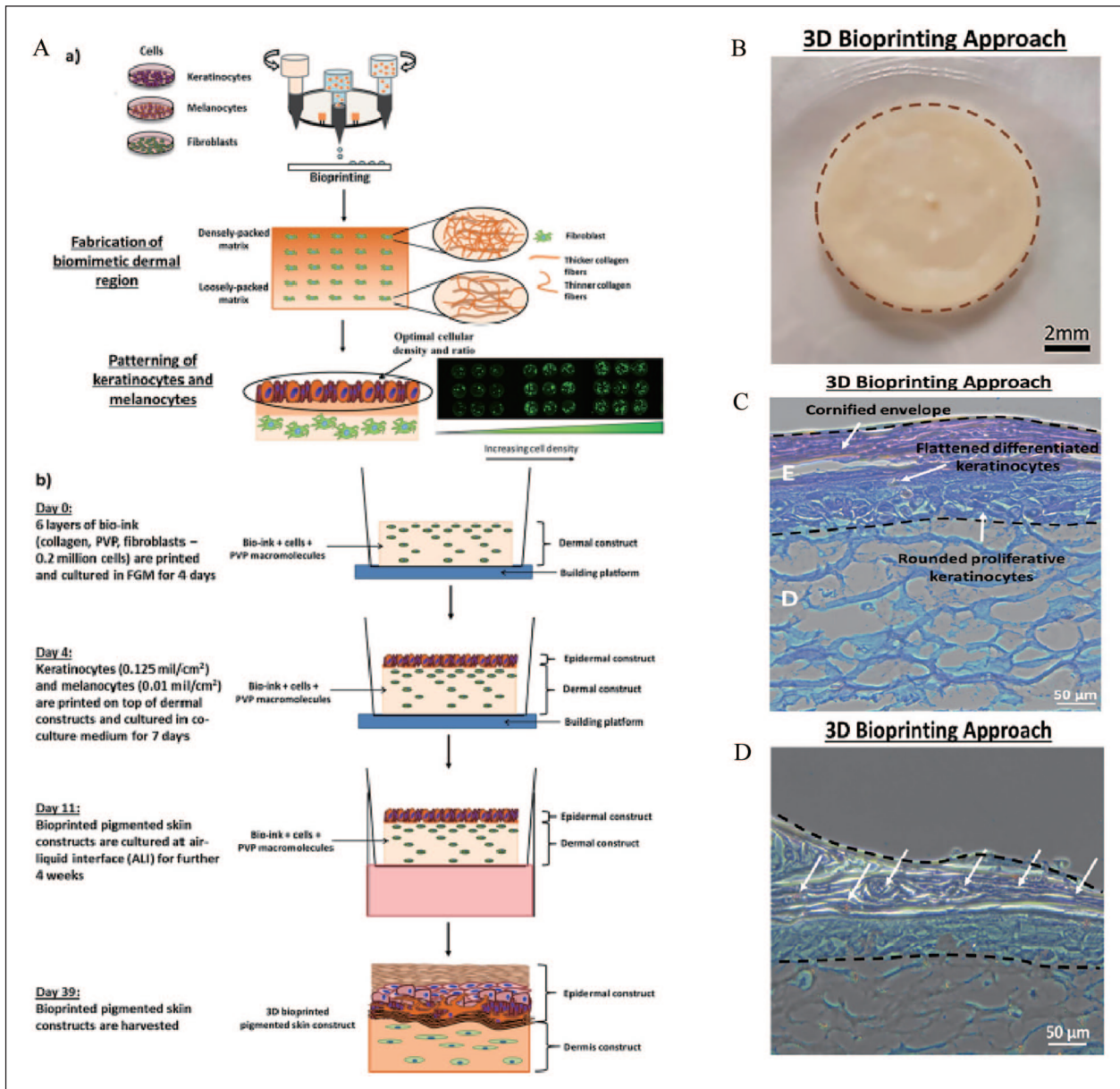


Figure 7. (A-a) Schematic drawing of a two-step bioprinting strategy for design and fabrication of 3D pigmented human skin constructs, (A-b) fabrication process for the 3D pigmented human skin constructs, (B) representative images of 3D pigmented human skin constructs fabricated via 3D bioprinting. 3D bioprinted pigmented human skin constructs with uniform skin pigmentation, pigmented area is enclosed by the brown dotted line. scale bar: 2 mm, (C) representative images of H&E staining of 3D pigmented human skin constructs. scale bar: 50 μm. The epidermal region is indicated by E and the dermal region is indicated by D, and (D) representative images of Fontana Masson staining of 3D pigmented human skin constructs. scale bar: 50 μm. Arrows indicating the distribution of melanin granules within the epidermal region of 3D matrices (stained brownish-black). Source: Adapted with permission from Ng et al.¹⁸⁵

of hair follicles in vivo and maintain the biological characteristics of HPCs and HFSCs to realize reconstruction of mature hair follicles in vitro. Higgins et al.¹⁹⁰ demonstrated that the intact dermal papilla transcriptional signature could be partially restored through the growth of papilla cells in 3D spheroid cultures. This signature change translated to a partial restoration of inductive capability, and induced de novo hair follicles in human skin. Miao et al.¹⁹¹ also prepared 3D-structured HPC spheres on a Matrigel

scaffold. HPC spheres showed marker gene expression characteristic of hair papilla [NCAM, Versican, and α -smooth muscle actin (α -SMA)], which are lost during 2D culture. Zhang et al.¹⁹² used a hair follicle regeneration model to evaluate the hair follicle-inducing ability of dermal papilla multicellular spheroids that formed on nanofiber sponge. Phosphate buffer solution (PBS) containing dermal papilla microtissues were injected into the dorsal hypodermis of nude mice. Experiments showed that

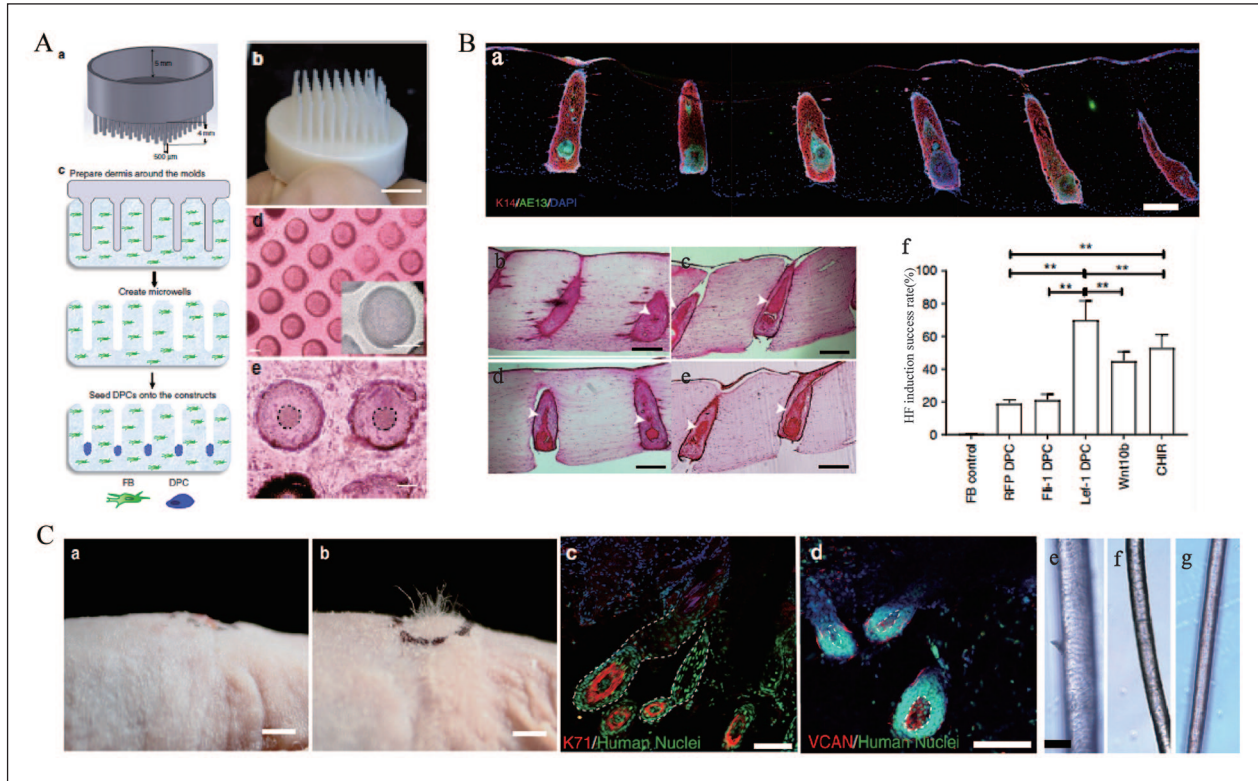


Figure 8. (A) Patterning of collagen type-I gel using 3D-printed molds allows for physiological arrangement of cells in the hair follicle. Hair follicle molds were designed (a) and 3D-printed (b), (c) the collagen gel containing dermal fibroblasts could solidify around the HF-like extensions to create an array of microwells in which the DPCs formed spontaneous aggregates, (d) top view of HSCs containing DPCs which settled down into the microwells (lower panel: higher magnification of the microwells), and (e) DPCs formed spontaneous aggregates at the center of the microwells (dashed line circles the aggregates). Scale bars for (d) and (e) are 100 μ m. (B) (a) Low magnification image demonstrating expression of AE13 in HSCs generated using Lef-1-transfected DPCs and the high efficiency in HF lineage differentiation, histological H&E staining of the constructs generated by empty vector-transfected DPCs (b), lef-1-transfected DPCs (c), Wnt10b-treated DPCs (d), and CHIR99021-treated DPCs (e) (arrows showing differentiated KC morphology), (f) success rate, defined as the ratio of the HFUs exhibiting hair follicle differentiation to the total number of HFUs, for HSCs with DPCs at different treatment conditions compared to FB control. Scale bars are 300 μ m. (C) (a) (as a control), (b) engraftment of high follicle-density HSCs onto immune-deficient nude mice led to hair growth in the grafts after 4–6 weeks (b), (c and d) human-specific nuclear staining (green) indicated that the de novo hair follicles marked with K71 (c) and DPCs marked with VCAN (d) are comprised of human cells. Bright-field microscopy of unpigmented terminal human hair (e), engineered human hair in the grafts (f), and unpigmented human vellus hair (g) showed morphological similarities between human hair and engineered hair. Scale bars for (a, b), (c–d), and (e–g) are 2 mm, 200 μ m, and 50 μ m respectively. Source: Adapted with permission from Abaci et al.¹⁹³

cultured dermal papilla multicellular spheroids could effectively enhance hair follicle-inducing ability.

In recent years, with breakthroughs in stem cell research and the development of 3D bioprinting technology, research on hair follicle regeneration using 3D bioprinting technology has advanced. Abaci et al.¹⁹³ developed a biomimetic approach for generation of human hair follicles within human skin constructs by recapitulating the physiological 3D organization of cells in the hair follicle microenvironment using 3D bioprinting technology. 3D bioprinting technology created the structures of human hair follicles with high aspect ratios, which was not possible using previous microfabrication techniques (Figure 8). Overexpression of Lef-1 in DPCs restores the intact DPC transcriptional signature and significantly enhances the efficiency of hair

follicle differentiation in human skin constructs. Feng et al.¹⁹⁴ used 3D bioprinting to print a hair follicle-like 3D structure containing epidermal cells and Fbs derived from the foreskin of children in the dermis layer of epidermal/dermal TES. The constructed TES was transplanted to the full-thickness skin defect on the back of nude mice, and white hair was visible after 3 weeks. Biological 3D printing for regenerating hair follicles requires a suitable microenvironment for hair follicle growth. This microenvironment can maintain the function of hair papilla cells. Biological 3D printing technology can simulate the microenvironment of hair follicles in vitro and induce hair follicle regeneration. Therefore, 3D bioprinting has provided new solutions for hair follicle regeneration and promoted the development of STE and regenerative medicine.

Bioprinting for sweat glands

Previous studies have successfully induced stem cells into functional sweat gland cells *in vitro* using a 3D bio-printed sweat gland development microenvironment. The stem cells used for sweat gland regeneration today mainly include ESCs, MSCs, bone marrow MSCs (BM-MSCs), and mammary progenitor cells (MPCs).

ESCs, as a source of sweat gland cell development *in vivo*, have advantages as seed cells in inducing sweat gland regeneration *in vitro*. Huang et al.⁷⁹ used 3D bioprinting technology to construct a 3D ECM *in vitro* with gelatin/alginate hydrogel as bioink. At the same time, mouse ESCs, plantar dermis homogenate, and EGF were incorporated into 3D ECM to simulate the microenvironment of sweat gland development. Finally, the hydrogel was placed on the burn wound of a mouse paw. The 3D ECM containing the above-mentioned cells continuously and slowly synthesized and released EGF and BMP4. Meanwhile, under the action of plantar dermal cells, epidermal stem cells differentiated into sweat gland cells on the 14th day after transplantation. Due to their ability for self-renewal and multipotent properties, MSCs have broad prospects in therapeutic TE and regenerative medicine.¹⁹⁵ Yao et al.¹⁹⁶ used alginate/gelatin hydrogel as bioink and adopted a 3D bioprinting technique to mimic the regenerative microenvironment that directed the specific sweat gland differentiation of MSCs and ultimately guided the formation and function of glandular tissue. Their findings demonstrated that directed differentiation of MSCs into sweat glands in a 3D-printed matrix both *in vitro* and *in vivo* was feasible. Bioprinting MSCs successfully repaired the damaged sweat glands *in vivo*, suggesting that it can improve the regenerative potential of exogenous differentiated MSCs. Furthermore, they identified that CTHRC1 and Hmox1 were critical biochemical regulators for sweat gland specification; CTHRC1 and Hmox1 synergistically boosted the sweat gland gene expression profile (Figure 9).

BM-MSCs have been used in stem cell therapy to help wound healing and skin appendage repair.^{197,198} Previous studies have confirmed that BM-MSCs can differentiate into sweat gland-like cells *in vitro* and develop secretory function after transplantation *in vivo*.^{198–200} Another studies have cultured mouse BM-MSCs in a sweat gland development microenvironment constructed *in vitro* and found that cells aggregated and proliferated into clusters.²⁰¹ The high expression of sweat gland-specific keratin and secretion-related genes was detected in cells. *In vivo* experiments have shown that the induced stem cells can promote the functional repair of sweat glands. The above experiments indicated that mouse BM-MSCs were successfully transformed into mouse functional sweat gland cells across lineages after being induced by the 3D bio-printed sweat gland microenvironment. Preliminary studies support a mechanism in which CTHRC1 protein in

mouse foot homogenate activates the EDA-Shh signaling pathway of sweat gland development during induction.

Mammary glands and sweat glands are both secretory organs with the same origin and have similar structure and cell type.²⁰² Studies have shown that mouse MPCs transplanted into salivary glands in mice can develop into salivary gland-like structures, indicating that differentiation of MPCs can be affected by changes in the microenvironment. Therefore, MPCs as a cell source have great potential in inducing sweat gland regeneration *in vitro*.^{203,204} Wang et al.²⁰⁵ explored the critical role of the engineered sweat gland microenvironment in reprogramming MPCs into functional sweat gland cells. They used a 3D sweat gland microenvironment composed of gelatin-alginate hydrogels and components from mouse sweat gland extracellular matrix proteins to reroute the differentiation of MPCs to study the functions of this microenvironment. MPCs were encapsulated into the artificial sweat gland microenvironment and were printed into a 3D cell-laden construct. Based on these results, MPCs encapsulated in the bioprinted 3D sweat gland microenvironment exhibited significant expression of the functional markers of mouse sweat glands. The differentiated mouse MPCs could regenerate sweat gland cells in the engineered sweat gland microenvironment *in vitro*. The Shh pathway was found to be correlated with changes in the differentiation. When the Shh pathway is inhibited, the expression of sweat gland-associated proteins in MPCs under the same induction environment is significantly reduced.

Although previous studies have successfully reprogrammed animal-derived stem cells into sweat gland cells using 3D bioprinting methods *in vitro*, their induction efficiency is relatively low. Transplantation rejection and the long-term safety of xenogeneic cells are the main obstacles that restrict the widespread application of sweat gland regeneration in clinic. The physical and chemical factors of the 3D sweat gland microenvironment constructed *in vitro* affects the efficiency of sweat gland regeneration, such as the hardness and degradation rate of the microenvironment. Therefore, identifying more suitable bioinks to simulate the microenvironment of sweat gland development is important.

Perspectives and challenges

3D bioprinting has the advantages of high resolution, flexible operation, repeatable printing, and high-throughput output. However, all technologies, including 3D bioprinting, suffer from certain limitations and pose challenges. First, there are still key technical problems that must be addressed in bioink: (1) Human skin has unique physical and mechanical characteristics, which makes it important to select biological materials corresponding to skin tissue characteristics in the process of skin 3D bioprinting. (2) The selected printing materials must be compatible with the 3D printing

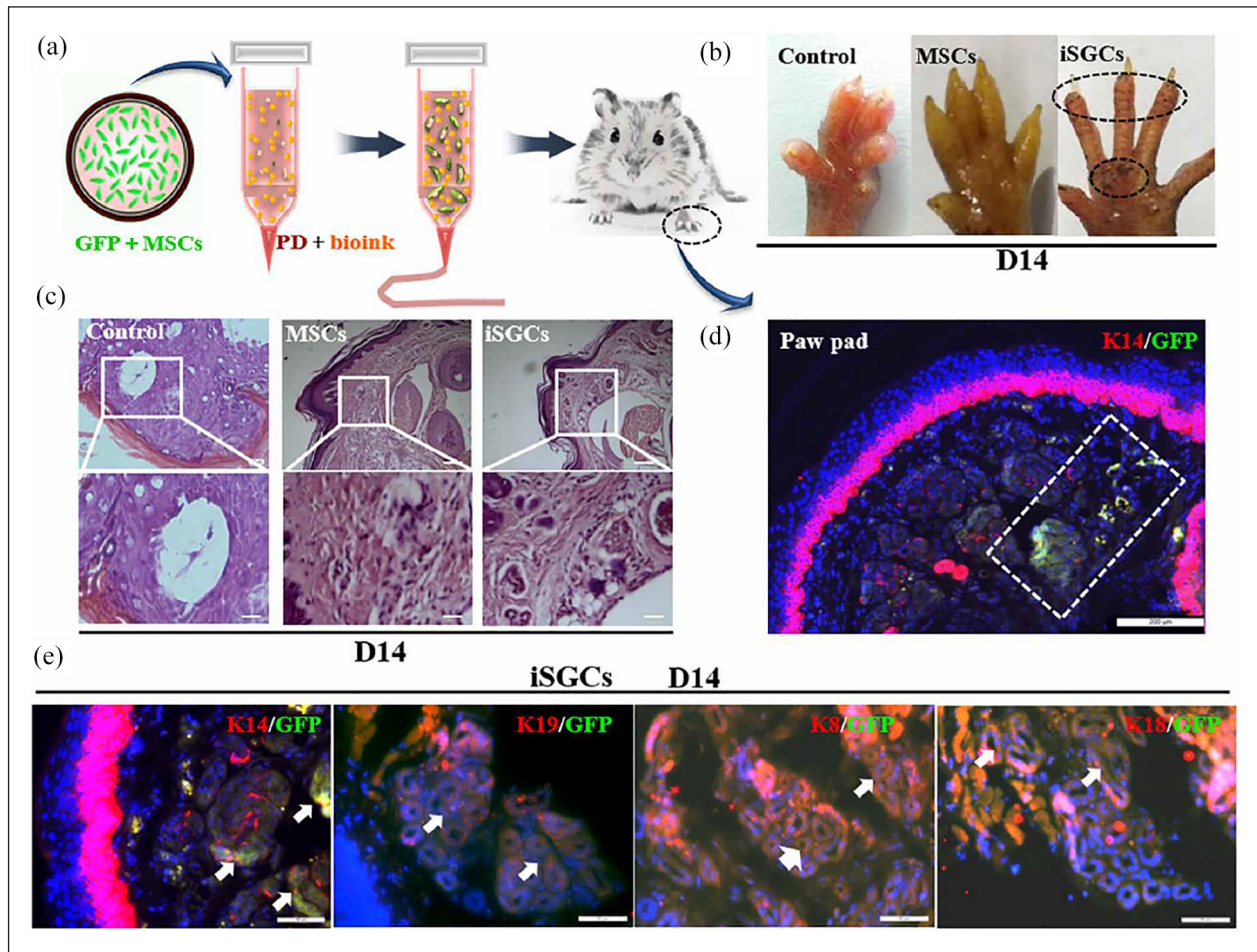


Figure 9. Directed regeneration of sweat gland (SG) in thermal-injured mouse model after transplantation of induced SG cells (iSGCs): (a) schematic illustration of approaches for engineering iSGCs and transplantation, (b) sweat test of mice treated with different cells, (c) histology of plantar region without treatment and transplantation of MSCs and iSGCs (scale bars, 200 μm), (d) involvement of GFP-labeled iSGCs in directed regeneration of SG tissue in thermal-injured mouse model (K14, red; GFP, green; DAPI, blue; scale bar, 200 μm), and (e) SG-specific markers K14, K19, K8, and K18 detected in regenerated SG tissue (arrows) (K14, K19, K8, and K18, red; GFP, green; scale bars, 50 μm).

Source: Adapted with permission from Yao et al.¹⁹⁶

system. Due to shrinkage or decreased strength of these materials after printing, they cannot meet the use requirements of 3D bioprinting. (3) The mechanical strength of 3D bioprinted hydrogels is insufficient, and maintenance of structural stability after compression is difficult. Therefore, it is important to identify a superior gelation method to achieve rapid and stable gelation of the pregelatinized solution without affecting cell viability. The research status of 3D bioprinting for TES indicates that an ideal bioink remains to be identified. In future, the material composition of bioink can be further optimized, such as by the introduction of nanomaterials, to improve the regeneration of tissues or organs.

3D-bioprinted skin tissue constructs cannot simulate the precise structure of skin (such as blood vessels, nerves, and skin appendages). Currently, printing skin structures with highly developed vasculature remains challenging.²⁰⁶ Nerve regeneration of 3D-printed skin is a challenging but interesting topic. During the process of 3D-printed skin-induced

neo-tissue formation, nerve regeneration is dependent on newly formed blood vessels. With a lack of blood supply, nerve regeneration is almost completely inhibited.²⁰⁷ Furthermore, Schwann cells play an important role in nerve regeneration.²⁰⁸ The roles of Schwann cells in promoting nerve regeneration include: (1) proliferation and aggregation to form a tubular structure similar to a “nerve conduit,” which induces the directional growth of nerve fibers, (2) synthesizing and secreting a large number of laminins, which promote nerve growth and can significantly accelerate the regeneration of class A nerve fibers,²⁰⁹ and (3) secretion of nerve growth factor and other neurotrophic factors to promote axon regeneration by upregulating the expression of neuronal cell adhesion molecules.²¹⁰ Hence, Schwann cells, as a key cellular component in skin sensory nerve regeneration, are added to the 3D printed scaffold in vitro, which is a good method for the regeneration of 3D-printing skin sensory nerves.

Finally, seed cells are also an important aspect to consider in 3D bioprinting technology. Stem cells have attracted a great deal of attention as an important source of tissue-engineered seed cells. Recent studies indicated that stem cells can play an important role in promoting skin appendage regeneration, wound healing, and tissue reconstruction.^{211–213} Stem cells have great potential in the field of TES, but ethical issues, costs, and technical requirements hinder the full use of stem cells. Although many studies have shown good prospects for the combination of 3D-printed skin and growth factors, research progress remains slow. There are a number of possible explanations for this: (1) growth factors are expensive and easy to deactivate, and have stringent storage, transportation, and production requirements, (2) the application and regulation of multiple growth factors remains challenging, and (3) the method of introducing growth factors into TE scaffolds involves a variety of chemical reagents, and their safety, effectiveness, and stability raise potential biosafety concerns. In addition, currently available 3D-printed skin is limited by long healing times and high cost. Although 3D bioprinting may significantly shorten healing time, cost should be considered.

The application of 3D bioprinting technology in the field of tissue repair and regeneration is feasible. The possibility of 3D bioprinting skin, thereby eliminating donor site morbidity associated with skin grafts, as well as creating in vitro tumor models such as malignant melanoma, could have significant health benefits.²¹⁴ It is possible to study cell proliferation, metastasis and chemotherapy drug detection by recapitulating the skin and skin cancer microenvironment with 3D bio-printing.²¹⁵ In the long term, 3D bioprinting, as a panacea, is able to directly print skin onto a wound caused by skin cancer excision, burns, could revolutionize the prognosis of patients.²¹⁶ So far, research in this field has shown that 3D bioprinting will allow for accurate placement of all the various native skin cell types and precisely reproducible fabrication of constructs to replace injured or wounded skin. However, reproducing the structural integrity and functionality of native skin to allow wound repair, temperature control, and sensation is yet to be achieved. With the progress of related technologies and the exploration of multidisciplinary cooperation, 3D bioprinting is expected to overcome these obstacles and play an important role in bioengineering and skin bionics.

Acknowledgements

The authors wish to thank Jie Zhang for her advice on the figures of this review.

Authors' contributions

TW and XW designed the major structure of this review. TW and XW conducted the search on related literature. TW, WZ, PW, YX, MY, RJ, SX, JW, HC, and XW were involved in the literature review. All authors were involving in drafting the article or

revising it critically for important intellectual content, and all authors approved the final version to be published. All authors read and approved the final manuscript.

Declaration of conflicting interests

The author(s) declared no potential conflicts of interest with respect to the research, authorship, and/or publication of this article.

Funding

The author(s) disclosed receipt of the following financial support for the research, authorship, and/or publication of this article: This work was financially supported by the National key research and development project (2016YFC1100800, 2016YFC1100803), the National Natural Science Foundation of China (81772069, 81401591, 81801911), and the Zhejiang Provincial Basic Public Welfare Research Program (LGF19H150008).

Availability of data and materials

All data or related information supporting the conclusions of the review is included in the article.

ORCID iD

Xingang Wang  <https://orcid.org/0000-0002-7522-7782>

References

1. Thompson CM, Hocking AM, Honari S, et al. Genetic risk factors for hypertrophic scar development. *J Burn Care Res* 2013; 34: 477–482.
2. Ai L and Weng L. Heat shock sweat gland cells induce phenotypic transformation of human bone marrow mesenchymal stem cells. *Chin J Tissue Eng Res* 2013;17: 985–991.
3. Groeber F, Holeiter M, Hampel M, et al. Skin tissue engineering—in vivo and in vitro applications. *Adv Drug Deliv Rev* 2011; 63: 352–366.
4. Novosel EC, Kleinhans C and Kluger PJ. Vascularization is the key challenge in tissue engineering. *Adv Drug Deliv Rev* 2011; 63: 300–311.
5. Huang S, Xu Y, Wu C, et al. In vitro constitution and in vivo implantation of engineered skin constructs with sweat glands. *Biomaterials* 2010; 31: 5520–5525.
6. Zimmerman A, Bai L and Ginty DD. The gentle touch receptors of mammalian skin. *Science* 2014; 346: 950–954.
7. Chuong CM, Randall VA, Widelitz RB, et al. Physiological regeneration of skin appendages and implications for regenerative medicine. *Physiology* 2012; 27: 61–72.
8. Zong X, Bien H, Chung CY, et al. Electrospun fine-textured scaffolds for heart tissue constructs. *Biomaterials* 2005; 26: 5330–5338.
9. Moroni L, de Wijn JR and van Blitterswijk CA. 3D fiber-deposited scaffolds for tissue engineering: influence of pores geometry and architecture on dynamic mechanical properties. *Biomaterials* 2006; 27: 974–985.
10. Bacakova M, Musilkova J, Riedel T, et al. The potential applications of fibrin-coated electrospun polylactide nanofibers in skin tissue engineering. *Int J Nanomed* 2016; 11: 771–789.

11. Vig K, Chaudhari A, Tripathi S, et al. Advances in skin regeneration using tissue engineering. *Int J Mol Sci* 2017; 18: 789.
12. Dong RH, Jia YX, Qin CC, et al. In situ deposition of a personalized nanofibrous dressing via a handy electrospinning device for skin wound care. *Nanoscale* 2016; 8: 3482–3488.
13. Liu GS, Yan X, Yan FF, et al. In situ electrospinning iodine-based fibrous meshes for antibacterial wound dressing. *Nanoscale Res Lett* 2018; 13: 309.
14. Duan GG, Jiang SH, Jerome V, et al. Ultralight, soft polymer sponges by self-assembly of short electrospun fibers in colloidal dispersions. *Adv Funct Mater* 2015; 25: 2850–2856.
15. Khalil S and Sun W. Bioprinting endothelial cells with alginate for 3D tissue constructs. *J Biomech Eng* 2009; 131: 111002.
16. Ozbolat IT and Yu Y. Bioprinting toward organ fabrication: challenges and future trends. *IEEE Trans Biomed Eng* 2013; 60: 691–699.
17. Seol YJ, Kang HW, Lee SJ, et al. Bioprinting technology and its applications. *Eur J Cardiothorac Surg* 2014; 46: 342–348.
18. Zhu W, Ma X, Gou M, et al. 3D printing of functional biomaterials for tissue engineering. *Curr Opin Biotechnol* 2016; 40: 103–112.
19. Knowlton S, Anand S, Shah T, et al. Bioprinting for neural tissue engineering. *Trends Neurosci* 2018; 41: 31–46.
20. Huang Y, Zhang XF, Gao G, et al. 3D bioprinting and the current applications in tissue engineering. *Biotechnol J* 2017; 12: 1600734.
21. Telser AG, Young JK and Baldwin KM. *Elsevier's integrated histology*. Philadelphia, PA: Mosby, Inc., 2007.
22. McLafferty E, Hendry C and Alistair F. The integumentary system: anatomy, physiology and function of skin. *Nurs Stand* 2012; 27: 35–42.
23. Kumar V, Abbas AK, Fausto N, et al. *Robbins basic pathology*. 8th ed. Philadelphia, PA: Saunders Elsevier, 2008.
24. Adkinson NF, Bochner BS, Burks AW, et al. *Middleton's allergy: principles and practice*. Philadelphia, PA: Saunders Elsevier, 2014.
25. Marks JG. *Lookingbill and Marks' principles of dermatology*. Philadelphia, PA: Elsevier Inc., 2013.
26. Jiang Y, Huang S, Fu X, et al. Epidemiology of chronic cutaneous wounds in China. *Wound Repair Regen* 2011; 19: 181–188.
27. Sun BK, Siprashvili Z and Khavari PA. Advances in skin grafting and treatment of cutaneous wounds. *Science* 2014; 346: 941–945.
28. Jahoda CA and Oliver RF. Vibrissa dermal papilla cell aggregative behaviour in vivo and in vitro. *J Embryol Exp Morphol* 1984; 79: 211–224.
29. Ma DR, Yang EN and Lee ST. A review: the location, molecular characterisation and multipotency of hair follicle epidermal stem cells. *Ann Acad Med Singapore* 2004; 33: 784–788.
30. Cotsarelis G. Epithelial stem cells: a folliculocentric view. *J Invest Dermatol* 2006; 126: 1459–1468.
31. Martin P. Wound healing—aiming for perfect skin regeneration. *Science* 1997; 276: 75–81.
32. Shibasaki M, Wilson TE and Crandall CG. Neural control and mechanisms of eccrine sweating during heat stress and exercise. *J Appl Physiol* 2006; 100: 1692–1701.
33. Li H, Chen L, Zhang M, et al. Three-dimensional culture and identification of human eccrine sweat glands in matrigel basement membrane matrix. *Cell Tissue Res* 2013; 354: 897–902.
34. Horie N, Yokozeki H and Sato K. Proteolytic enzymes in human eccrine sweat: a screening study. *Am J Physiol* 1986; 250: R691–R698.
35. Reitamo S, Anttila HSI, Didierjean L, et al. Immunohistochemical identification of interleukin-I-alpha and interleukin-I-beta in human eccrine sweat-gland apparatus. *Brit J Dermatol* 1990; 122: 315–323.
36. Sato K and Sato F. Interleukin-1-alpha in human sweat is functionally active and derived from the eccrine sweat gland. *Am J Physiol* 1994; 266: R950–R959.
37. Lu C and Fuchs E. Sweat gland progenitors in development, homeostasis, and wound repair. *Cold Spring Harb Perspect Med* 2014; 4: a015222.
38. James WD, Berger TG and Elston DM. *Andrews' diseases of the skin clinical dermatology*. 11th ed. Philadelphia, PA: Elsevier Inc., 2011.
39. Fitzpatrick JE and Morelli JG. *Dermatology secrets plus*. 4th ed. Philadelphia, PA: Mosby, Inc., 2011.
40. Choi HI, Sohn KC, Hong DK, et al. Melanosome uptake is associated with the proliferation and differentiation of keratinocytes. *Arch Dermatol Res* 2014; 306: 59–66.
41. Chung H, Jung H, Lee JH, et al. Keratinocyte-derived laminin-332 protein promotes melanin synthesis via regulation of tyrosine uptake. *J Biol Chem* 2014; 289: 21751–21759.
42. Gu BK, Choi DJ, Park SJ, et al. 3D bioprinting technologies for tissue engineering applications. *Adv Exp Med Biol* 2018; 1078: 15–28.
43. Arslan-Yildiz A, El Assal R, Chen P, et al. Towards artificial tissue models: past, present, and future of 3D bioprinting. *Biofabrication* 2016; 8: 014103.
44. Gudapati H, Dey M and Ozbolat I. A comprehensive review on droplet-based bioprinting: past, present and future. *Biomaterials* 2016; 102: 20–42.
45. Derby B. Inkjet printing of functional and structural materials: fluid property requirements, feature stability, and resolution. *Annu Rev Mater Res* 2010; 40: 395–414.
46. Saunders RE and Derby B. Inkjet printing biomaterials for tissue engineering: bioprinting. *Int Mater Revi* 2014; 59: 430–448.
47. Binder KW, Zhao W, Aboushwareb T, et al. In situ bioprinting of the skin for burns. *J Am Coll Surg* 2010; 211: S76.
48. Ozbolat IT and Hospodiuk M. Current advances and future perspectives in extrusion-based bioprinting. *Biomaterials* 2016; 76: 321–343.
49. Onses MS, Sutanto E, Ferreira PM, et al. Mechanisms, capabilities, and applications of high-resolution electrohydrodynamic jet printing. *Small* 2015; 11: 4237–4266.
50. Jayasinghe SN and Townsend-Nicholson A. Stable electric-field driven cone-jetting of concentrated biosuspensions. *Lab Chip* 2006; 6: 1086–1090.
51. Kim HS, Lee DY, Park JH, et al. Optimization of electrohydrodynamic writing technique to print collagen. *Exp Tech* 2007; 31: 15–19.

52. Workman VL, Tezera LB, Elkington PT, et al. Controlled generation of microspheres incorporating extracellular matrix fibrils for three-dimensional cell culture. *Adv Funct Mater* 2014; 24: 2648–2657.
53. Jayasinghe SN, Qureshi AN and Eagles PA. Electrohydrodynamic jet processing: an advanced electric-field-driven jetting phenomenon for processing living cells. *Small* 2006; 2: 216–219.
54. Koch L, Gruene M, Unger C, et al. Laser assisted cell printing. *Curr Pharm Biotechnol* 2013; 14: 91–97.
55. Guillemot F, Souquet A, Catros S, et al. Laser-assisted cell printing: principle, physical parameters versus cell fate and perspectives in tissue engineering. *Nanomedicine* 2010; 5: 507–515.
56. Ringeisen BR, Othon CM, Barron JA, et al. Jet-based methods to print living cells. *Biotechnol J* 2006; 1: 930–948.
57. Devillard R, Pages E, Correa MM, et al. Cell patterning by laser-assisted bioprinting. *Methods Cell Biol* 2014; 119: 159–174.
58. Michael S, Sorg H, Peck CT, et al. Tissue engineered skin substitutes created by laser-assisted bioprinting form skin-like structures in the dorsal skin fold chamber in mice. *PLoS One* 2013; 8: e57741.
59. Koch L, Kuhn S, Sorg H, et al. Laser printing of skin cells and human stem cells. *Tissue Eng Part C Methods* 2010; 16: 847–854.
60. Serra P, Duocastella M, Fernández-Pradas JM, et al. Liquids microprinting through laser-induced forward transfer. *Appl Surf Sci* 2009; 255: 5342–5345.
61. Patrascioiu A, Fernández-Pradas JM, Palla PA, et al. Laser-generated liquid microjets: correlation between bubble dynamics and liquid ejection. *Microfluid Nanofluidics* 2014; 16: 55–63.
62. Ali M, Pages E, Ducom AA, et al. Controlling laser-induced jet formation for bioprinting mesenchymal stem cells with high viability and high resolution. *Biofabrication* 2014; 6: 045001.
63. Mironov V, Boland T, Trusk T, et al. Organ printing: computer-aided jet-based 3D tissue engineering. *Trends Biotechnol* 2003; 21: 157–161.
64. Shafiee A and Atala A. Printing technologies for medical applications. *Trends Mol Med* 2016; 22: 254–265.
65. Fielding GA, Bandyopadhyay A and Bose S. Effects of silica and zinc oxide doping on mechanical and biological properties of 3D printed tricalcium phosphate tissue engineering scaffolds. *Dent Mater* 2012; 28: 113–122.
66. Nguyen NT, John JS, Kamble H, et al. Three-dimensional printing of biological matters. *J Sci Adv Mater Devices* 2016; 1: 17.
67. Matai I, Kaur G, Seyedsalehi A, et al. Progress in 3D bioprinting technology for tissue/organ regenerative engineering. *Biomaterials* 2020; 226: 119536.
68. Liu W, Zhang YS, Heinrich MA, et al. Rapid continuous multimaterial extrusion bioprinting. *Adv Mater* 2017; 29: 1604630.
69. Dhariwala B, Hunt E and Boland T. Rapid prototyping of tissue-engineering constructs, using photopolymerizable hydrogels and stereolithography. *Tissue Eng* 2004; 10: 1316–1322.
70. Melchels FP, Feijen J and Grijpma DW. A review on stereolithography and its applications in biomedical engineering. *Biomaterials* 2010; 31: 6121–6130.
71. Heinrich MA, Liu W, Jimenez A, et al. 3D Bioprinting: from benches to translational applications. *Small* 2019; 15: e1805510.
72. Zhu W, Qu X, Zhu J, et al. Direct 3D bioprinting of prevascularized tissue constructs with complex micro-architecture. *Biomaterials* 2017; 124: 106–115.
73. Varkey M, Visscher DO, van Zuijlen PPM, et al. Skin bioprinting: the future of burn wound reconstruction? *Burns Trauma* 2019; 7: 4.
74. Li J, Chen M, Fan X, et al. Recent advances in bioprinting techniques: approaches, applications and future prospects. *J Transl Med* 2016; 14: 271.
75. Choi WS, Ha D, Park S, et al. Synthetic multicellular cell-to-cell communication in inkjet printed bacterial cell systems. *Biomaterials* 2011; 32: 2500–2507.
76. Cui X and Boland T. Human microvasculature fabrication using thermal inkjet printing technology. *Biomaterials* 2009; 30: 6221–6227.
77. Yanez M, Rincon J, Dones A, et al. In vivo assessment of printed microvasculature in a bilayer skin graft to treat full-thickness wounds. *Tissue Eng Part A* 2015; 21: 224–233.
78. Ng WL, Yeong WY and Naing MW. Development of polyelectrolyte chitosan gelatin hydrogels for skin bioprinting. *Procedia CIRP* 2016; 49: 105–112.
79. Huang S, Yao B, Xie JF, et al. 3D bioprinted extracellular matrix mimics facilitate directed differentiation of epithelial progenitors for sweat gland regeneration. *Acta Biomater* 2016; 32: 170–177.
80. Tirella A, Orsini A, Vozzi G, et al. A phase diagram for microfabrication of geometrically controlled hydrogel scaffolds. *Biofabrication* 2009; 1: 045002.
81. Murphy SV, Skardal A and Atala A. Evaluation of hydrogels for bio-printing applications. *J Biomed Mater Res A* 2013; 101: 272–284.
82. Kopf M, Campos DF, Blaeser A, et al. A tailored three-dimensionally printable agarose-collagen blend allows encapsulation, spreading, and attachment of human umbilical artery smooth muscle cells. *Biofabrication* 2016; 8: 025011.
83. Sun J and Tan H. Alginate-based biomaterials for regenerative medicine applications. *Materials* 2013; 6: 1285–1309.
84. Glicklis R, Shapiro L, Agbaria R, et al. Hepatocyte behavior within three-dimensional porous alginate scaffolds. *Biotech Bioeng* 2000; 67: 344–353.
85. Guillemot F, Souquet A, Catros S, et al. High-throughput laser printing of cells and biomaterials for tissue engineering. *Acta Biomater* 2010; 6: 2494–2500.
86. Axpe E and Oyen ML. Applications of alginate based bioinks in 3D bioprinting. *Int J Mol Sci* 2016; 17: 1976.
87. Chandy T and Sharma CP. Chitosan-as a biomaterial. *Biomater Artif Cells Artif Organs* 1990; 18: 1–24.
88. Munaz A, Vadivelu RK, St., John J, et al. Three dimensional printing of biological matters. *J Sci Adv Mater Dev* 2016; 1: 1–17.
89. Livesey SA, Herndon DN, Hollyoak MA, et al. Transplanted acellular allograft dermal matrix. Potential

- as a template for the reconstruction of viable dermis. *Transplantation* 1995; 60: 1–9.
90. Ngo MD, Aberman HM, Hawes ML, et al. Evaluation of human acellular dermis versus porcine acellular dermis in an in vivo model for incisional hernia repair. *Cell Tissue Bank* 2011; 12: 135–145.
 91. Janis JE and Nahabedian MY. Acellular dermal matrices in surgery. *Plast Reconstr Surg* 2012; 130: 7S–8S.
 92. Ventura RD, Padalhin AR, Park CM, et al. Enhanced decellularization technique of porcine dermal ECM for tissue engineering applications. *Mater Sci Eng C* 2019; 104: 109841.
 93. Khan U and Bayat A. Microarchitectural analysis of decellularised unscarred and scarred dermis provides insight into the organisation and ultrastructure of the human skin with implications for future dermal substitute scaffold design. *J Tissue Eng* 2019; 10: 2041731419843710.
 94. Leng L, Ma J, Sun X, et al. Comprehensive proteomic atlas of skin biomatrix scaffolds reveals a supportive microenvironment for epidermal development. *J Tissue Eng* 2020; 11: 2041731420972310.
 95. Ahn G, Min KH, Kim C, et al. Precise stacking of decellularized extracellular matrix based 3D cell-laden constructs by a 3D cell printing system equipped with heating modules. *Sci Rep* 2017; 7: 8624.
 96. Seidlits SK, Khaing ZZ, Petersen RR, et al. The effects of hyaluronic acid hydrogels with tunable mechanical properties on neural progenitor cell differentiation. *Biomaterials* 2010; 31: 3930–3940.
 97. Murakami K, Aoki H, Nakamura S, et al. Hydrogel blends of chitin/chitosan, fucoidan and alginate as healing-impaired wound dressings. *Biomaterials* 2010; 31: 83–90.
 98. Kim GH, Ahn SH, Kim YY, et al. Coaxial structured collagen–alginate scaffolds: fabrication, physical properties, and biomedical application for skin tissue regeneration. *J Mater Chem* 2011; 21: 6165–6172.
 99. Mao JS, Cui YL, Wang XH, et al. A preliminary study on chitosan and gelatin polyelectrolyte complex cytocompatibility by cell cycle and apoptosis analysis. *Biomaterials* 2004; 25: 3973–3981.
 100. Ma L, Gao C, Mao Z, et al. Collagen/chitosan porous scaffolds with improved biostability for skin tissue engineering. *Biomaterials* 2003; 24: 4833–4841.
 101. Shi H, Han C, Mao Z, et al. Enhanced angiogenesis in porous collagen-chitosan scaffolds loaded with angiogenin. *Tissue Eng Part A* 2008; 14: 1775–1785.
 102. Mota C, Puppi D, Chiellini F, et al. Additive manufacturing techniques for the production of tissue engineering constructs. *J Tissue Eng Regen Med* 2015; 9: 174–190.
 103. Aboudzadeh N, Imani M, Shokrgozar MA, et al. Fabrication and characterization of poly(D,L-lactide-co-glycolide)/hydroxyapatite nanocomposite scaffolds for bone tissue regeneration. *J Biomed Mater Res A* 2010; 94: 137–145.
 104. Jansen J, Melchels FPW, Grijpma DW, et al. Fumaric acid monoethyl ester-functionalized poly(D,L-lactide)/N-vinyl-2-pyrrolidone resins for the preparation of tissue engineering scaffolds by stereolithography. *Biomacromolecules* 2009; 10: 214–220.
 105. Rogina A, Pribolsan L, Hanzek A, et al. Macroporous poly(lactic acid) construct supporting the osteoinductive porous chitosan-based hydrogel for bone tissue engineering. *Polymer* 2016; 98: 172–181.
 106. Wu L and Ding J. In vitro degradation of three-dimensional porous poly(D,L-lactide-co-glycolide) scaffolds for tissue engineering. *Biomaterials* 2004; 25: 5821–5830.
 107. Agrawal CM and Ray RB. Biodegradable polymeric scaffolds for musculoskeletal tissue engineering. *J Biomed Mater Res* 2001; 55: 141–150.
 108. Wang X, You C, Hu X, et al. The roles of knitted mesh-reinforced collagen-chitosan hybrid scaffold in the one-step repair of full-thickness skin defects in rats. *Acta Biomater* 2013; 9: 7822–7832.
 109. Gumusderelioglu M, Dalkiranoglu S, Aydin RS, et al. A novel dermal substitute based on biofunctionalized electrospun PCL nanofibrous matrix. *J Biomed Mater Res A* 2011; 98: 461–472.
 110. Siddiqui N, Asawa S, Birru B, et al. PCL-based composite scaffold matrices for tissue engineering applications. *Mol Biotechnol* 2018; 60: 506–532.
 111. You Y, Min BM, Lee SJ, et al. In vitro degradation behavior of electrospun polyglycolide, polylactide, and poly(lactide-co-glycolide). *J Appl Polym Sci* 2004; 95: 193–200.
 112. Kim HS, Chen J, Wu LP, et al. Prevention of excessive scar formation using nanofibrous meshes made of biodegradable elastomer poly(3-hydroxybutyrate-co-3-hydroxyvalerate). *J Tissue Eng* 2020; 11: 2041731420949332.
 113. Yue K, Trujillo-de Santiago G, Alvarez MM, et al. Synthesis, properties, and biomedical applications of gelatin methacryloyl (GelMA) hydrogels. *Biomaterials* 2015; 73: 254–271.
 114. Nichol JW, Koshy ST, Bae H, et al. Cell-laden micro-engineered gelatin methacrylate hydrogels. *Biomaterials* 2010; 31: 5536–5544.
 115. Zhang Y, Ouyang H, Lim CT, et al. Electrospinning of gelatin fibers and gelatin/PCL composite fibrous scaffolds. *J Biomed Mater Res B Appl Biomater* 2005; 72: 156–165.
 116. Chong EJ, Phan TT, Lim IJ, et al. Evaluation of electrospun PCL/gelatin nanofibrous scaffold for wound healing and layered dermal reconstitution. *Acta Biomater* 2007; 3: 321–330.
 117. Fee T, Surianarayanan S, Downs C, et al. Nanofiber alignment regulates NIH3T3 cell orientation and cytoskeletal gene expression on electrospun PCL+gelatin nanofibers. *PLoS One* 2016; 11: e0154806.
 118. Dias JR, Baptista-Silva S, Sousa A, et al. Biomechanical performance of hybrid electrospun structures for skin regeneration. *Mater Sci Eng C* 2018; 93: 816–827.
 119. Pal P, Dadhich P, Srivas PK, et al. Bilayered nanofibrous 3D hierarchy as skin rudiment by emulsion electrospinning for burn wound management. *Biomater Sci* 2017; 5: 1786–1799.
 120. Wang X, Li Q, Hu X, et al. Fabrication and characterization of poly(L-lactide-co-glycolide) knitted mesh-reinforced collagen-chitosan hybrid scaffolds for dermal tissue engineering. *J Mech Behav Biomed Mater* 2012; 8: 204–215.
 121. Wang X, Han C, Hu X, et al. Applications of knitted mesh fabrication techniques to scaffolds for tissue engineering and regenerative medicine. *J Mech Behav Biomed Mater* 2011; 4: 922–932.

122. Xiao S, Zhao T, Wang J, et al. Gelatin methacrylate (GelMA)-based hydrogels for cell transplantation: an effective strategy for tissue engineering. *Stem Cell Rev Rep* 2019; 15: 664–679.
123. Schuurman W, Levett PA, Pot MW, et al. Gelatin-methacrylamide hydrogels as potential biomaterials for fabrication of tissue-engineered cartilage constructs. *Macromol Biosci* 2013; 13: 551–561.
124. Strateffeffen H, Kopf M, Kreimendahl F, et al. GelMA-collagen blends enable drop-on-demand 3D printability and promote angiogenesis. *Biofabrication* 2017; 9: 045002.
125. Shi Y, Xing TL, Zhang HB, et al. Tyrosinase-doped bioink for 3D bioprinting of living skin constructs. *Biomed Mater* 2018; 13: 035008.
126. el-Ghalbzouri A, Gibbs S, Lamme E, et al. Effect of fibroblasts on epidermal regeneration. *Br J Dermatol* 2002; 147: 230–243.
127. Sorrell JM and Caplan AI. Fibroblast heterogeneity: more than skin deep. *J Cell Sci* 2004; 117: 667–675.
128. Driskell RR and Watt FM. Understanding fibroblast heterogeneity in the skin. *Trends Cell Biol* 2015; 25: 92–99.
129. Zuo Y, Yu X and Lu S. Dermal fibroblasts from different layers of pig skin exhibit different profibrotic and morphological characteristics. *Anat Rec* 2016; 299: 1585–1599.
130. Driskell RR, Lichtenberger BM, Hoste E, et al. Distinct fibroblast lineages determine dermal architecture in skin development and repair. *Nature* 2013; 504: 277–281.
131. Habif TP. *Clinical dermatology: a color guide to diagnosis and therapy*. 5th ed. Hanover, NH: Elsevier Inc., 2010.
132. Bologna JL, Jorizzo JL and Schaffer JV. *Dermatology*. 3rd ed. London: Elsevier Limited, 2012.
133. Chen S, Liu B, Carlson MA, et al. Recent advances in electrospun nanofibers for wound healing. *Nanomedicine* 2017; 12: 1335–1352.
134. Sheikh FA, Ju HW, Lee JM, et al. 3D electrospun silk fibroin nanofibers for fabrication of artificial skin. *Nanomedicine* 2015; 11: 681–691.
135. Mahjour SB, Fu X, Yang X, et al. Rapid creation of skin substitutes from human skin cells and biomimetic nanofibers for acute full-thickness wound repair. *Burns* 2015; 41: 1764–1774.
136. Abaci HE, Guo Z, Coffman A, et al. Human skin constructs with spatially controlled vasculature using primary and iPSC-derived endothelial cells. *Adv Healthc Mater* 2016; 5: 1800–1807.
137. Kerouredan O, Bourget JM, Remy M, et al. Micropatterning of endothelial cells to create a capillary-like network with defined architecture by laser-assisted bioprinting. *J Mater Sci Mater Med* 2019; 30: 28.
138. Liu Y, Suwa F, Wang XW, et al. Reconstruction of a tissue-engineered skin containing melanocytes. *Cell Biol Int* 2007; 31: 985–990.
139. Nishimura EK. Melanocyte stem cells: a melanocyte reservoir in hair follicles for hair and skin pigmentation. *Pigment Cell Melanoma Res* 2011; 24: 401–410.
140. Tumber T, Guasch G, Greco V, et al. Defining the epithelial stem cell niche in skin. *Science* 2004; 303: 359–363.
141. Yang CC and Cotsarelis G. Review of hair follicle dermal cells. *J Dermatol Sci* 2010; 57: 2–11.
142. Huang SP, Huang CH, Shyu JF, et al. Promotion of wound healing using adipose-derived stem cells in radiation ulcer of a rat model. *J Biomed Sci* 2013; 20: 51.
143. Maxson S, Lopez EA, Yoo D, et al. Concise review: role of mesenchymal stem cells in wound repair. *Stem Cells Transl Med* 2012; 1: 142–149.
144. Moorefield EC, McKee EE, Solchaga L, et al. Cloned, CD117 selected human amniotic fluid stem cells are capable of modulating the immune response. *PLoS One* 2011; 6: e26535.
145. De Coppi P, Bartsch G, Jr, Siddiqui MM, et al. Isolation of amniotic stem cell lines with potential for therapy. *Nat Biotechnol* 2007; 25: 100–106.
146. Skardal A, Mack D, Kapetanovic E, et al. Bioprinted amniotic fluid-derived stem cells accelerate healing of large skin wounds. *Stem Cells Transl Med* 2012; 1: 792–802.
147. Aasen T, Raya A, Barrero MJ, et al. Efficient and rapid generation of induced pluripotent stem cells from human keratinocytes. *Nat Biotechnol* 2008; 26: 1276–1284.
148. Smith AS, Macadangang J, Leung W, et al. Human iPSC-derived cardiomyocytes and tissue engineering strategies for disease modeling and drug screening. *Biotechnol Adv* 2017; 35: 77–94.
149. Laato M, Niinikoski J, Lebel L, et al. Stimulation of wound healing by epidermal growth factor. A dose-dependent effect. *Ann Surg* 1986; 203: 379–381.
150. Gainza G, Bonafonte DC, Moreno B, et al. The topical administration of rhEGF-loaded nanostructured lipid carriers (rhEGF-NLC) improves healing in a porcine full-thickness excisional wound model. *J Control Release* 2015; 197: 41–47.
151. Chen JD, Kim JP, Zhang K, et al. Epidermal growth factor (EGF) promotes human keratinocyte locomotion on collagen by increasing the alpha 2 integrin subunit. *Exp Cell Res* 1993; 209: 216–223.
152. Ando Y and Jensen PJ. Epidermal growth factor and insulin-like growth factor I enhance keratinocyte migration. *J Invest Dermatol* 1993; 100: 633–639.
153. Tiede S, Ernst N, Bayat A, et al. Basic fibroblast growth factor: a potential new therapeutic tool for the treatment of hypertrophic and keloid scars. *Ann Anat* 2009; 191: 33–44.
154. Wu J, Ye J, Zhu J, et al. Heparin-based coacervate of FGF2 improves dermal regeneration by asserting a synergistic role with cell proliferation and endogenous facilitated VEGF for cutaneous wound healing. *Biomacromolecules* 2016; 17: 2168–2177.
155. Claffey KP, Abrams K, Shih SC, et al. Fibroblast growth factor 2 activation of stromal cell vascular endothelial growth factor expression and angiogenesis. *Lab Invest* 2001; 81: 61–75.
156. Xiong S, Zhang X, Lu P, et al. A gelatin-sulfonated silk composite scaffold based on 3D printing technology enhances skin regeneration by stimulating epidermal growth and dermal neovascularization. *Sci Rep* 2017; 7: 4288.
157. Mironov V. The second international workshop on bioprinting, biopatterning and bioassembly. *Expert Opin Biol Ther* 2005; 5: 1111–1115.

158. Duncan CO, Shelton RM, Navsaria H, et al. In vitro transfer of keratinocytes: comparison of transfer from fibrin membrane and delivery by aerosol spray. *J Biomed Mater Res B Appl Biomater* 2005; 73: 221–228.
159. Robert AW, Azevedo Gomes F, Rode MP, et al. The skin regeneration potential of a pro-angiogenic secretome from human skin-derived multipotent stromal cells. *J Tissue Eng* 2019; 10: 2041731419833391.
160. Kirchmajer DM, Gorkin R and Panhuis MIH. An overview of the suitability of hydrogel-forming polymers for extrusion-based 3D-printing. *J Mater Chem B* 2015; 3: 4105–4117.
161. Ng WL, Yeong WY and Naing MW. Polyelectrolyte gelatin-chitosan hydrogel optimized for 3D bioprinting in skin tissue engineering. *Int J Bioprinting* 2016; 2: 53–62.
162. Lee V, Singh G, Trasatti JP, et al. Design and fabrication of human skin by three-dimensional bioprinting. *Tissue Eng Part C Methods* 2014; 20: 473–484.
163. Cubo N, Garcia M, Del Canizo JF, et al. 3D bioprinting of functional human skin: production and in vivo analysis. *Biofabrication* 2016; 9: 015006.
164. Wang S, Xiong Y, Chen J, et al. Three dimensional printing bilayer membrane scaffold promotes wound healing. *Front Bioeng Biotechnol* 2019; 7: 348.
165. Lee W, Debasitis JC, Lee VK, et al. Multi-layered culture of human skin fibroblasts and keratinocytes through three-dimensional freeform fabrication. *Biomaterials* 2009; 30: 1587–1595.
166. Ozbolat IT. Bioprinting scale-up tissue and organ constructs for transplantation. *Trends Biotechnol* 2015; 33: 395–400.
167. Binder KW. *In situ bioprinting of the skin*. PhD Dissertation, Ann Arbor, Wake Forest University Graduate School of Arts and Sciences, 2011.
168. Albanna M, Binder KW, Murphy SV, et al. In situ bioprinting of autologous skin cells accelerates wound healing of extensive excisional full-thickness wounds. *Sci Rep* 2019; 9: 1856.
169. Rhodes M. *Inside L'Oreal's plan to 3D print human skin*. Fort Mill, South Carolina: First Research Industry Profiles, 2017.
170. Vijayavenkataraman S, Lu WF and Fuh JY. 3D bioprinting of skin: a state-of-the-art review on modelling, materials, and processes. *Biofabrication* 2016; 8: 032001.
171. Jain RK, Au P, Tam J, et al. Engineering vascularized tissue. *Nat Biotechnol* 2005; 23: 821–823.
172. Huling J, Ko IK, Atala A, et al. Fabrication of biomimetic vascular scaffolds for 3D tissue constructs using vascular corrosion casts. *Acta Biomater* 2016; 32: 190–197.
173. Kang HW, Lee SJ, Ko IK, et al. A 3D bioprinting system to produce human-scale tissue constructs with structural integrity. *Nat Biotechnol* 2016; 34: 312–319.
174. Bourget JM, Kerouredan O, Medina M, et al. Patterning of endothelial cells and mesenchymal stem cells by laser-assisted bioprinting to study cell migration. *Biomed Res Int* 2016; 2016: 3569843.
175. Chouhan D, Dey N, Bhardwaj N, et al. Emerging and innovative approaches for wound healing and skin regeneration: current status and advances. *Biomaterials* 2019; 216: 119267.
176. Richardson TP, Peters MC, Ennett AB, et al. Polymeric system for dual growth factor delivery. *Nat Biotechnol* 2001; 19: 1029–1034.
177. Chen RR, Silva EA, Yuen WW, et al. Spatio-temporal VEGF and PDGF delivery patterns blood vessel formation and maturation. *Pharm Res* 2007; 24: 258–264.
178. Cui H, Zhu W, Nowicki M, et al. Hierarchical fabrication of engineered vascularized bone biphasic constructs via dual 3D bioprinting: integrating regional bioactive factors into architectural design. *Adv Healthc Mater* 2016; 5: 2174–2181.
179. Mori N, Morimoto Y and Takeuchi S. Skin integrated with perfusable vascular channels on a chip. *Biomaterials* 2017; 116: 48–56.
180. Kolesky DB, Truby RL, Gladman AS, et al. 3D Bioprinting of vascularized, heterogeneous cell-laden tissue constructs. *Adv Mater* 2014; 26: 3124–3130.
181. Bertassoni LE, Cecconi M, Manoharan V, et al. Hydrogel bioprinted microchannel networks for vascularization of tissue engineering constructs. *Lab Chip* 2014; 14: 2202–2211.
182. Kim BS, Lee JS, Gao G, et al. Direct 3D cell-printing of human skin with functional transwell system. *Biofabrication* 2017; 9: 025034.
183. Kim BS, Gao G, Kim JY, et al. 3D Cell printing of perfusable vascularized human skin equivalent composed of epidermis, dermis, and hypodermis for better structural recapitulation of native skin. *Adv Healthc Mater* 2019; 8: e1801019.
184. Min D, Lee W, Bae IH, et al. Bioprinting of biomimetic skin containing melanocytes. *Exp Dermatol* 2018; 27: 453–459.
185. Ng WL, Qi JTZ, Yeong WY, et al. Proof-of-concept: 3D bioprinting of pigmented human skin constructs. *Biofabrication* 2018; 10: 025005.
186. Wu JJ, Zhu TY, Lu YG, et al. Hair follicle reformation induced by dermal papilla cells from human scalp skin. *Arch Dermatol Res* 2006; 298: 183–190.
187. Li S, Hu M and Lorenz HP. Treatment of full-thickness skin wounds with blood-derived CD34(+) precursor cells enhances healing with hair follicle regeneration. *Adv Wound Care* 2020; 9: 264–276.
188. Weng T, Wu P, Zhang W, et al. Regeneration of skin appendages and nerves: current status and further challenges. *J Transl Med* 2020; 18: 53.
189. Sriwiriyanont P, Lynch KA, Maier EA, et al. Morphogenesis of chimeric hair follicles in engineered skin substitutes with human keratinocytes and murine dermal papilla cells. *Exp Dermatol* 2012; 21: 783–785.
190. Higgins CA, Chen JC, Cerise JE, et al. Microenvironmental reprogramming by three-dimensional culture enables dermal papilla cells to induce de novo human hair-follicle growth. *Proc Natl Acad Sci U S A* 2013; 110: 19679–19688.
191. Miao Y, Sun YB, Liu BC, et al. Controllable production of transplantable adult human high-passage dermal papilla spheroids using 3D matrigel culture. *Tissue Eng Part A* 2014; 20: 2329–2338.
192. Zhang K, Bai X, Yuan Z, et al. Cellular nanofiber structure with secretory activity-promoting characteristics for

- multicellular spheroid formation and hair follicle regeneration. *ACS Appl Mater Interfaces* 2020; 12: 7931–7941.
193. Abaci HE, Coffman A, Doucet Y, et al. Tissue engineering of human hair follicles using a biomimetic developmental approach. *Nat Commun* 2018; 9: 5301.
194. Feng S. *The construction of tissue engineering skin with the capability of hair growth*. Ann Arbor: Peking Union Medical College, 2017.
195. Keating A. Mesenchymal stromal cells: new directions. *Cell Stem Cell* 2012; 10: 709–716.
196. Yao B, Wang R, Wang Y, et al. Biochemical and structural cues of 3D-printed matrix synergistically direct MSC differentiation for functional sweat gland regeneration. *Sci Adv* 2020; 6: eaaz1094.
197. Xu Y, Huang S, Ma K, et al. Promising new potential for mesenchymal stem cells derived from human umbilical cord Wharton's jelly: sweat gland cell-like differentiative capacity. *J Tissue Eng Regen Med* 2012; 6: 645–654.
198. Xu Y, Hong Y, Xu M, et al. Role of keratinocyte growth factor in the differentiation of sweat gland-like cells from human umbilical cord-derived mesenchymal stem cells. *Stem Cells Transl Med* 2016; 5: 106–116.
199. Sheng Z, Fu X, Cai S, et al. Regeneration of functional sweat gland-like structures by transplanted differentiated bone marrow mesenchymal stem cells. *Wound Repair Regen* 2009; 17: 427–435.
200. Xu Y, Huang S and Fu X. Autologous transplantation of bone marrow-derived mesenchymal stem cells: a promising therapeutic strategy for prevention of skin-graft contraction. *Clin Exp Dermatol* 2012; 37: 497–500.
201. Kolakshyapati P, Li X, Chen C, et al. Gene-activated matrix/bone marrow-derived mesenchymal stem cells constructs regenerate sweat glands-like structure in vivo. *Sci Rep* 2017; 7: 17630.
202. Inman JL, Robertson C, Mott JD, et al. Mammary gland development: cell fate specification, stem cells and the microenvironment. *Development* 2015; 142: 1028–1042.
203. Sakakura T, Nishizuka Y and Dawe CJ. Mesenchyme-dependent morphogenesis and epithelium-specific cytodifferentiation in mouse mammary gland. *Science* 1976; 194: 1439–1441.
204. Cunha GR, Young P, Christov K, et al. Mammary phenotypic expression induced in epidermal cells by embryonic mammary mesenchyme. *Acta Anat* 1995; 152: 195–204.
205. Wang R, Wang Y, Yao B, et al. Redirecting differentiation of mammary progenitor cells by 3D bioprinted sweat gland microenvironment. *Burns Trauma* 2019; 7: 29.
206. Hendrickx B, Vranckx JJ and Lutun A. Cell-based vascularization strategies for skin tissue engineering. *Tissue Eng Part B Rev* 2011; 17: 13–24.
207. Gu XH, Terenghi G, Kangesu T, et al. Regeneration pattern of blood vessels and nerves in cultured keratinocyte grafts assessed by confocal laser scanning microscopy. *Br J Dermatol* 1995; 132: 376–383.
208. Bhatheja K and Field J. Schwann cells: origins and role in axonal maintenance and regeneration. *Int J Biochem Cell Biol* 2006; 38: 1995–1999.
209. Caissie R, Gingras M, Champigny MF, et al. In vivo enhancement of sensory perception recovery in a tissue-engineered skin enriched with laminin. *Biomaterials* 2006; 27: 2988–2993.
210. Friedlander DR, Grumet M and Edelman GM. Nerve growth factor enhances expression of neuron-glia cell adhesion molecule in PC12 cells. *J Cell Biol* 1986; 102: 413–419.
211. Zhou H, You C, Wang X, et al. The progress and challenges for dermal regeneration in tissue engineering. *J Biomed Mater Res A* 2017; 105: 1208–1218.
212. Xie J, Yao B, Han Y, et al. Skin appendage-derived stem cells: cell biology and potential for wound repair. *Burns Trauma* 2016; 4: 38.
213. Maranda EL, Rodriguez-Menocal L and Badiavas EV. Role of mesenchymal stem cells in dermal repair in burns and diabetic wounds. *Curr Stem Cell Res Ther* 2017; 12: 61–70.
214. Asghar W, El Assal R, Shafiee H, et al. Engineering cancer microenvironments for in vitro 3-D tumor models. *Mater Today* 2015; 18: 539–553.
215. Vultur A, Schanstra T and Herlyn M. The promise of 3D skin and melanoma cell bioprinting. *Melanoma Res* 2016; 26: 205–206.
216. Supp DM and Boyce ST. Engineered skin substitutes: practices and potentials. *Clin Dermatol* 2005; 23: 403–412.